

Discovery and Optimization of Novel Hydrogen Peroxide Activated Aromatic Nitrogen Mustard Derivatives as Highly Potent Anticancer Agents

WENBING CHEN, Heli Fan, Kumudha Balakrishnan, Yibin Wang, Huabing Sun, Yukai Fan, Varsha Gandhi, Leggy A. Arnold, and Xiaohua Peng

J. Med. Chem., **Just Accepted Manuscript** • DOI: 10.1021/acs.jmedchem.8b00559 • Publication Date (Web): 24 Sep 2018

Downloaded from <http://pubs.acs.org> on September 25, 2018

Just Accepted

"Just Accepted" manuscripts have been peer-reviewed and accepted for publication. They are posted online prior to technical editing, formatting for publication and author proofing. The American Chemical Society provides "Just Accepted" as a service to the research community to expedite the dissemination of scientific material as soon as possible after acceptance. "Just Accepted" manuscripts appear in full in PDF format accompanied by an HTML abstract. "Just Accepted" manuscripts have been fully peer reviewed, but should not be considered the official version of record. They are citable by the Digital Object Identifier (DOI®). "Just Accepted" is an optional service offered to authors. Therefore, the "Just Accepted" Web site may not include all articles that will be published in the journal. After a manuscript is technically edited and formatted, it will be removed from the "Just Accepted" Web site and published as an ASAP article. Note that technical editing may introduce minor changes to the manuscript text and/or graphics which could affect content, and all legal disclaimers and ethical guidelines that apply to the journal pertain. ACS cannot be held responsible for errors or consequences arising from the use of information contained in these "Just Accepted" manuscripts.



Discovery and Optimization of Novel Hydrogen Peroxide Activated Aromatic Nitrogen Mustard Derivatives as Highly Potent Anticancer Agents

Wenbing Chen ^{a,+}, Heli Fan ^{a,+}, Kumudha Balakrishnan^b, Yibin Wang, Huabing Sun, Yukai Fan, Varsha Gandhi^b, Leggy A. Arnold^a, and Xiaohua Peng^{a,*}

^aDepartment of Chemistry and Biochemistry and the Milwaukee Institute for Drug Discovery, University of Wisconsin Milwaukee, 3210 N. Cramer St., Milwaukee. WI 53211, USA.

^bDepartment of Experimental Therapeutics, MD Anderson Cancer Center, Houston, TX 77030, USA.

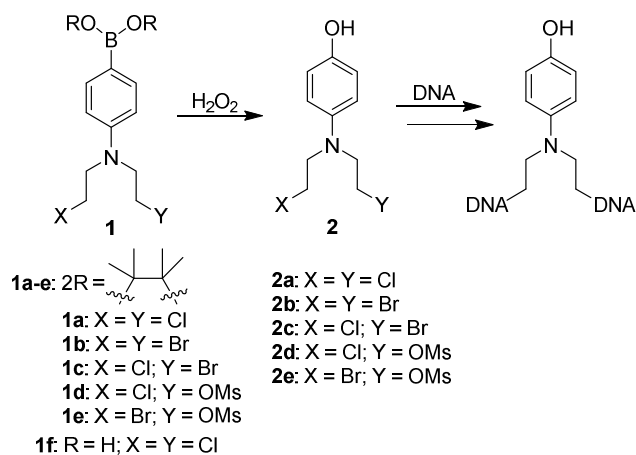
Keywords: ROS-activation; DNA cross-linking agents; reactive oxygen species; arylboronate esters; targeted anticancer drugs

ABSTRACT

We describe several new aromatic nitrogen mustards with various aromatic substituents and boronic ester that can be activated with H₂O₂ to efficiently cross-link DNA. *In vitro* studies demonstrated the anticancer potential of these compounds at lower concentrations than clinically used chemotherapeutics such as melphalan and chlorambucil. Especially compound **10** bearing an amino acid ester chain is selectively cytotoxic towards breast cancer and leukemia cells that inherently have high level of reactive oxygen species. Importantly, **10** was 10-14 fold more efficacious than melphalan and chlorambucil for triple negative breast cancer (TNBC) cells. Similarly, **10** is more toxic toward primary CLL cells than chlorambucil and the lead compound **9**. The introduction of an amino acid side chain improved the solubility and permeability of **10**. Furthermore, **10** inhibited the growth of TNBC tumors of xenografted mice without obvious signs of general toxicity making this compound an ideal drug candidate for clinical development.

INTRODUCTION

DNA cross-linking occurs when various exogenous or endogenous compounds connect two different positions of DNA.^{1,2} This reaction either takes place within the same DNA strand or at opposite strands, blocking DNA replication and in turn causing cell cycle arrest and cell death. DNA-cross-linking agents are effective against rapidly dividing cancer cells. However, many normal cells also divide very quickly, such as bone marrow, the lining of the mouth and intestines, and the hair follicles. Most clinically useful alkylating agents, such as cyclophosphamide, bendamustine, melphalan, and chlorambucil, have serious side effects. Thus, new potent alkylating agents with improved selectivity and reduced adverse effects are needed. DNA cross-linking agents that are induced under specific physiological conditions have the potential to reduce toxicity as these agents are not active by themselves but require specific conditions for activation. So far, numerous methods have been developed for inducing DNA cross-link formation under various conditions. Among the existing methods, photoirradiation,³⁻¹¹ reduction,¹²⁻¹⁷ oxidation,¹⁸⁻²¹ or fluoride induction²²⁻²⁴ are well studied and proved to be highly efficient. For example, Greenberg and Zhou's group employed phenyl selenide precursors for producing DNA interstrand cross-link (ICL) formation under mild oxidative conditions.¹⁸⁻²¹ Rokita and co-workers discovered several quinone methide precursors that induced DNA cross-linking in the presence of fluoride salts.^{22,23} The Freccero group introduced photogeneration of bifunctional quinone methides by laser flash photolysis.^{3,5,6,10,25} Gates and co-workers discovered hypoxia-selective DNA-alkylating agents built by grafting nitrogen mustards onto tirapazamine.¹⁶ A series of dinitrobenzamide nitrogen mustard reagents with a nitril-amidogen linker undergoes bioreduction to form DNA cross-links.¹²⁻¹⁵ Recently, our group has shown that the aryl boronic acids and esters are ideal trigger units for developing H₂O₂-activated DNA cross-linking agents.²⁶⁻³² Among these inducible DNA cross-linking agents, several classes of compounds showed anticancer activity and selectivity^{12,13,28,30}.



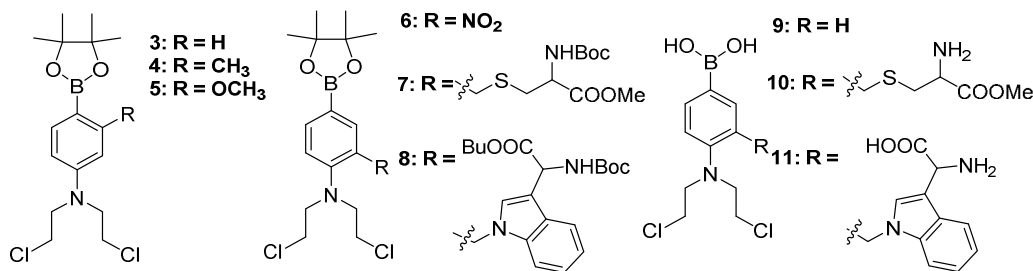
Scheme 1. H₂O₂-activated alkylating agents

Compared with their normal counterparts, most cancer cells have increased levels of reactive oxygen species (ROS) such as superoxide, H₂O₂, and hydroxyl radicals,³³⁻³⁵ which offers a possible way to develop selective anticancer agents. Pinacol boronate esters and boronic acids are excellent trigger groups responsive to hydrogen peroxide.³⁶ Our group discovered the first example of ROS-activated DNA alkylating agents with selective toxicity toward particular cancer cells.^{28,30} Although ROS-activated anticancer reagents have been sought for some time, very few agents effective *in vivo* have been developed so far.³⁷⁻³⁹ Aromatic nitrogen mustards are powerful DNA cross-linking agents. In particular, structure **1** (**1a-f**) with various leaving groups in the nitrogen mustard exhibit potent cellular activity, and selectively kill primary leukemic lymphocytes isolated from chronic lymphocytic leukemia patients (40–80% apoptosis) over normal lymphocytes from healthy donors (20% apoptosis). In this work, we modified **1a** and **1f** to develop analogues with increased anticancer activity by introducing different substituents on the aromatic ring. Several analogues of **1f** have been identified to be more toxic towards cancer cells than clinically used chemotherapy drugs. One of which (**10**) showed much higher activity than the lead compound (**9**). More importantly, *in vivo* efficacy was evaluated in a triple negative breast cancer xenograft mouse model with the results that **10** exhibited excellent antitumor properties.

RESULTS AND DISCUSSION

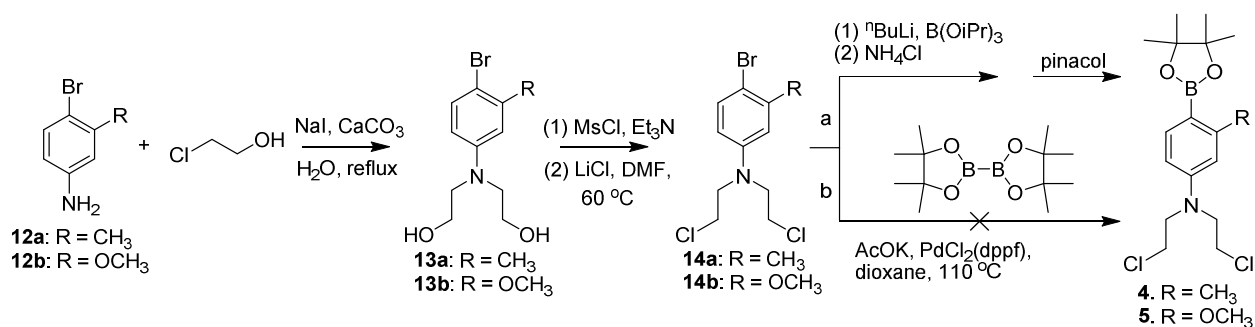
Chemistry. We modified aromatic nitrogen mustard **3** to identify more efficacious prodrugs. Therefore, ring

substitution patterns and pinacol boronate ester groups were investigated. Eight compounds (**4-11**) were designed and synthesized, which contained either a boronic acid group or a pinacol boronate ester as a H₂O₂-responsive trigger in combination with a nitrogen mustard as a DNA cross-linker (Scheme 2). Both electron donating (**4** and **5**) and withdrawing groups (**6**) were introduced for investigating the electronic effects in regard to their biological activity. Several amino acid side chains (**7**, **8**, **10**, and **11**) and pinacol boronate groups were employed to improve the biophysical and biochemical properties of these reagents.



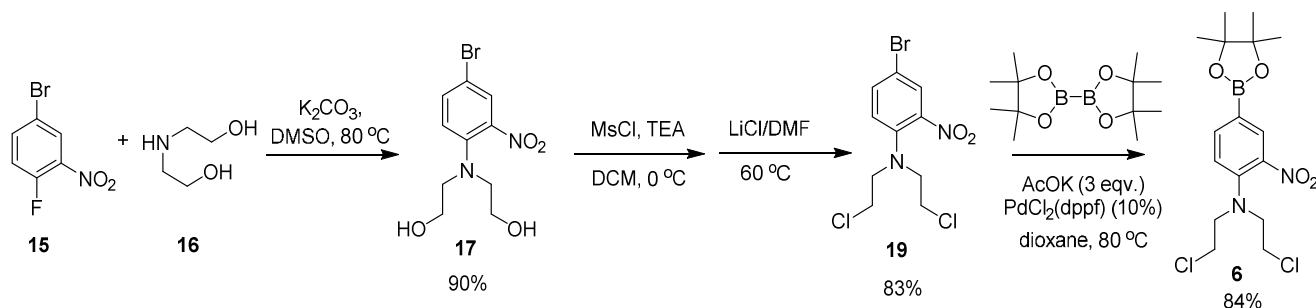
Scheme 2. Chemical structures of compounds **3-11**.

Compounds **4** and **5** were synthesized starting from ortho-substituted *p*-bromoaniline (**12a, b**) (Scheme 3). Alkylation of the amino group was performed with 2-chloroethanol in the presence of sodium iodide and calcium carbonate yielding **13a** and **13b**. Dichloromustards **14a** and **14b** were prepared from **13a** and **13b** via mesylation followed by chlorination. Classic palladium-catalyzed borylation of **14a** or **14b** did not produce the desired products (Scheme 3, path b). Thus, an alternative borylation strategy was employed involving the synthesis of the boronic acid analogues and subsequent esterification (Scheme 3, path a). Reaction of **14a** or **14b** with butyllithium and triisopropyl borate followed by hydrolysis yielded boronic acid derivatives, which were converted into the desired products **4** and **5** by esterification in the presence of pinacol and magnesium sulfate.

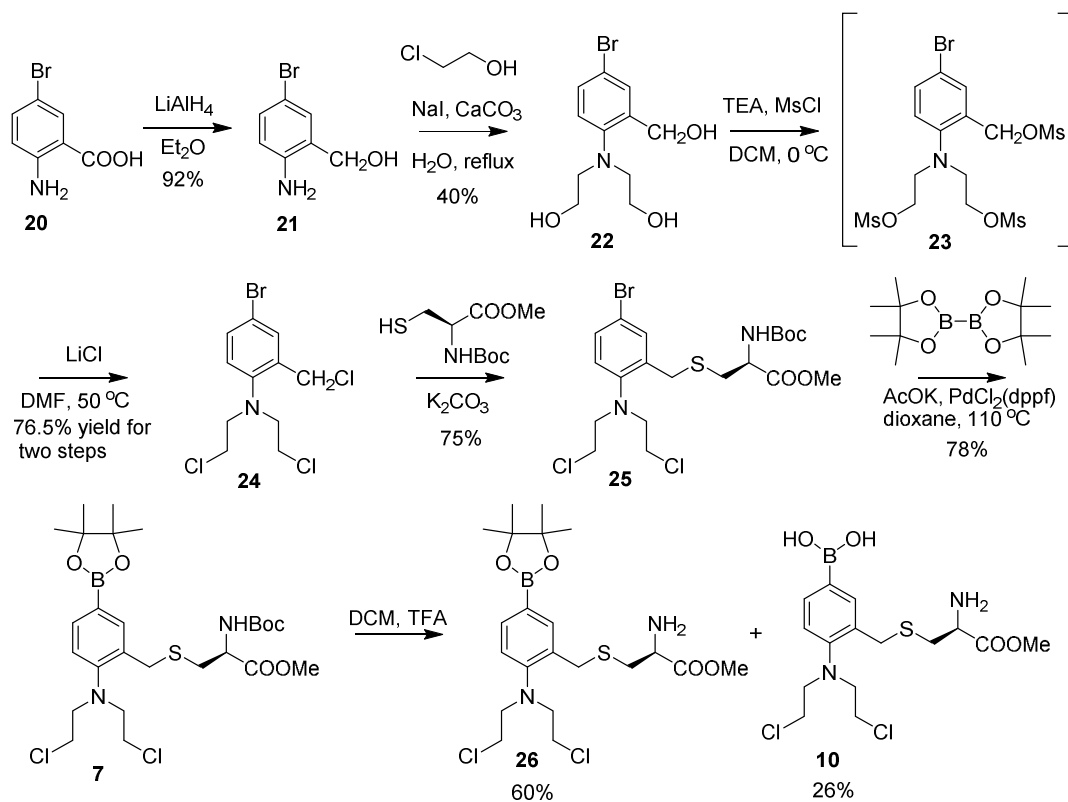


Scheme 3. Synthesis of compounds 4 and 5

Compound **6** was synthesized according to Scheme 4. Nucleophilic substitution of 4-bromo-1-fluoro-2-nitrobenzene **15** with diethanolamine (**16**) generated diol **17** with 90% yield. The hydroxyl groups of **17** were converted to a mesylate and replaced by chlorine using LiCl to yield nitro-substituted aromatic nitrogen mustard **19** in 80% yield for two steps. Finally, the desired product **6** was obtained by classic palladium-catalyzed borylation of **19**.

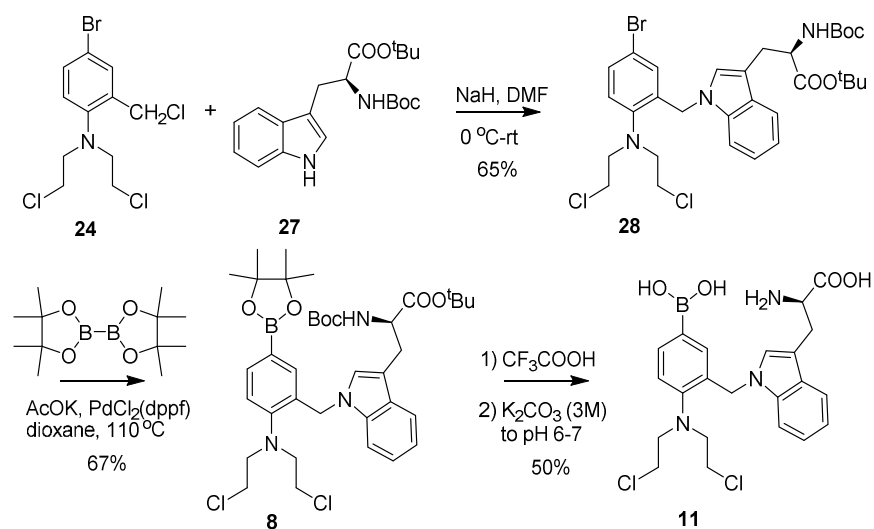
**Scheme 4. Synthesis of compound 6.**

Compounds **7** and **10** with a cysteine methyl ester chain were synthesized from benzoic acid derivative **20**. Reduction of **20** by lithium aluminum hydride yielded the corresponding hydroxymethyl analogue **21**. Similar to the synthesis of **14**, compound **21** was converted to the nitrogen mustard analogue **24** by *N*-alkylation (\rightarrow **22**), mesylation (\rightarrow **23**), and chlorination (\rightarrow **24**). In comparison with **12a** and **12b**, compound **21** was obtained in a lower yield (40%) and required a longer reaction time (3 days) for *N*-alkylation possibly due to the presence of an ortho-hydroxymethyl group that dramatically decreasing the nucleophilicity of the amino group. The cysteine methyl ester was selectively introduced at the benzylic position of **24** using one equivalent of *N*-*tert*-butoxycarbonyl cysteine methyl ester leading to **25**. Borylation of **25** generated **7** that in turn was deprotected with TFA providing the boronic acid ester **26** and the boronic acid **10**.



Scheme 5. Synthesis of compounds **7** and **10**.

Similarly, a tryptophan side chain was selectively introduced at the benzylic position of **24** with *N*-*tert*-butoxycarbonyl tryptophan ester **27** and sodium hydride as a base generating **28**. Subsequent borylation of **28** yielded the boronic acid ester **8**, which was converted to **11** by using TFA for deprotection and hydrolysis.



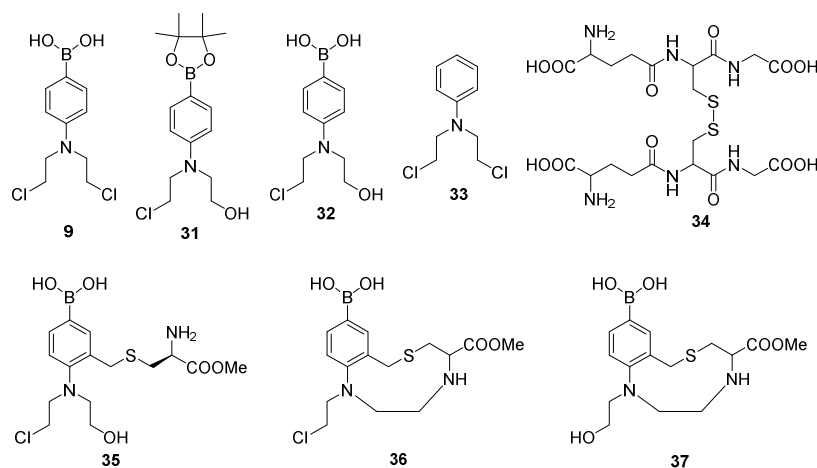
Scheme 6. Synthesis of compounds **8** and **11**.

Stability of the lead compounds. The stability is an essential factor of quality, safety, and efficacy of a drug product. Initially, the chemical stability of these ROS-activated DNA alkylating agents were determined in phosphate buffered saline (PBS) at physiological pH (7.4) and endosomal pH (6.0) as well as in the presence of GSH. The lead compounds **3**, **9**, and **10** were chosen for this study. To ensure the solubility of all compounds, a mixture of DMSO-d₆/PBS buffer was used. PBS buffer with pH 6.0 or pH 7.4 was prepared in D₂O, then diluted with DMSO-d₆ (the ratio of DMSO-d₆/PBS is 9:1) to provide the final buffer solution. A solution of 10 mM **3**, **9**, or **10** in 100 mM PBS buffer was incubated at room temperature for 3 to 10 days and monitored by NMR analysis (Figure S1A-C). Both **9** and **10** have good stability under the test conditions. After two days, >99% of **9** and 92% of **10** remained unchanged under both conditions (pH 6.0 and pH 7.4, respectively). There was still 99% of **9** and 85% of **10** remained undecomposed after incubation at rt for 4 days. Although compound **3** is less stable than **9** and **10**, it was mainly hydrolyzed to **9** in PBS buffer. Hydrolysis of **3** was complete within 48 hours.

Glutathione (GSH) is an important antioxidant in plants and animals. It is also a strong nucleophile that may compete with DNA to react with nitrogen mustards, therefore affecting the stability of these molecules. Thus, we further investigate the stability of **9** and **10** in the presence of GSH. Initially, a mixture of **9** or **10** and GSH with a ratio of 1:2 were incubated in DMSO-d₆/PBS buffer (9:1, pH 6.0). 90% DMSO was used because of poor solubility of **9** and **10** in phosphate buffer. For better comparison, two control samples with compound or GSH only were prepared. The results showed that the stability of **9** and **10** in the presence of GSH was similar to that in the absence of GSH (Figure S1D,E), indicating that GSH did not affect the stability of these compounds. Considering that DMSO may deactivate GSH, a lower percentage of DMSO (DMSO-d₆/PBS buffer 1:1) was used for the stability study of **9** and **10**. When DMSO percentage decreased to lower than 50%, **9** and **10** could not dissolve well, leading to a suspension. The results showed that the addition of GSH didn't affect the stability of **9** and **10** in 1:1 DMSO-d₆/PBS buffer. However, we did observe decreased stability of **9** and **10** in a solvent mixture with higher percentage of PBS buffer (50%)

(Figure S1F,G). In addition, compound **10** is less stable than **9**. More than 96% of **9** remained unchanged after 48 h incubation, while about 90% of **10** remained undecomposed after 24 h incubation and 70% undecomposed after 48 h incubation. Based on these results, we conclude that these ROS-activated DNA alkylating agents are relatively stable under cellular conditions as well as in the presence of GSH.

In order to further investigate the reactivity of these compounds at molecular level, the reaction mixture of **3**, **9**, and **10** after incubation in DMSO-d₆/PBS buffer at rt for 10 days was analyzed by IT-TOF mass analysis. Compounds **9** and **31** were detected from compound **3**, which was caused by hydrolysis (Scheme 7 and Scheme S3). Similarly, the hydrolysis product **32** was observed for **9**. In addition to **32**, deboronation product **33** was also formed. GSH was converted to its oxide form **34** after 10 days incubation. For **10**, apart from the hydrolysis product **35**, the adducts (**36** and **37**) caused by intramolecular attack were observed. Similar adducts were observed with or without the addition of GSH. No adducts were formed between GSH and **9** or **10**. These results provide the evidence for that GSH does not affect the stability of these H₂O₂-activated nitrogen mustard analogues.



Scheme 7. The proposed structure for the adducts generated from **3**, **9**, or **10** after incubation in PBS buffer for 10 days.

DNA cross-linking assay. The primary mechanism for the cytotoxicity of nitrogen mustard reagents entails

DNA ICL formation.^{1,2} ICLs are deleterious to cells, because they inhibit DNA replication and transcription. Additionally, it has been reported that cancer cells have higher levels of hydrogen peroxide than normal cells.^{33-35,40-44} Therefore, the mode of action of the synthesized reagents can be evaluated by their ability to induce DNA cross-links or DNA alkylations in the presence or absence of H₂O₂. In this work, the DNA cross-linking and selectivity of **3-11** were investigated using a 49-mer DNA duplex **30** that contained one consensus sequence for nitrogen mustards. ICL formation and yields were analyzed via denaturing polyacrylamide gel electrophoresis (PAGE) with phosphor image analysis (Image Quant 5.2).

5'-dGCCTAGTTCCTTTTAATTAAGTTCGCAATGCAAGTAATTAAGCTTGATCTG(**30a**)
 3'-dCGGATCAAGAAAATTAATGAACGTTACGTTTCATTAATTCGAACTAGAC(**30b**)

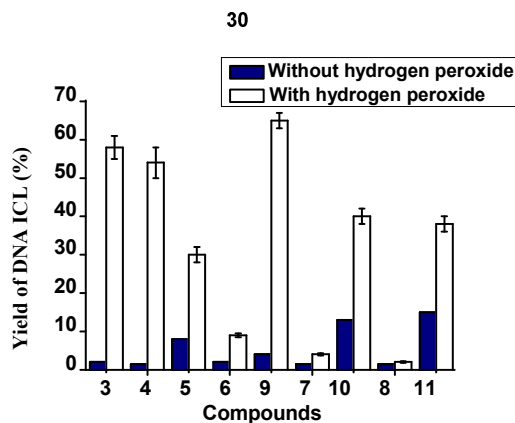


Figure 1. Comparison of the H₂O₂-induced activity and selectivity of **3-11**. The DNA cross-linking yields of these compounds were determined by treatment of a ³²P-labelled 49 mer DNA duplex with **3-11** (1.0 mM) in the presence or absence of H₂O₂ (1.5 mM) at room temperature for 16 h, then subjected to 20% denaturing PAGE analysis.

As expected, most compounds (**3-6** and **9-11**, 1.0 mM) in the absence of H₂O₂ (1.5 mM) induced very few DNA ICL formation (1.5 -15%), while addition of H₂O₂ greatly enhanced their cross-linking yields (up to 65%) (Figure 1 and Figure S2). Compounds with weak donating group such as (**4**) increased the selectivity (defined as the ratio of DNA ICL yield with H₂O₂ to that without H₂O₂). In contrast, compounds with strong donating group (**5**) or strong withdrawing group (**6**) decreased this ratio (Figure 1). A strong donating group offsets the deactivating effect of the boronic acid or ester group leading to increased cross-linking yield (8% for **5**) in the absence of H₂O₂. A withdrawing group suppresses the reactivity of the liberated compound

1 causing low enhancement on the H₂O₂-induced cross-linking efficiency (9% for **6**). These results suggested
2 that electronic effects can tune the cross-linking ability and selectivity of the compounds. We also
3 investigated compounds with amino acid side chains (**7**, **8**, **10** and **11**). Surprisingly, very low DNA ICL
4 yields (less than 5%) were observed for **7** and **8** either with or without H₂O₂. The low DNA cross-linking
5 capability might have been caused by steric hindrance of the BOC group that prevented **7** and **8** from
6 effectively interacting with major or minor grooves of DNA. Further investigation showed that removal of the
7 BOC group (**10** or **11**) lead to compounds with greatly enhanced DNA ICL formation. Thus, in addition to
8 electronic properties, steric hindrance greatly affect ICL formation of these compounds. The results further
9 indicated that a strong electron donating group or an amino acid side chain (**5**, **10**, and **11**) slightly increased
10 the DNA ICL yield in the absence of H₂O₂.
11
12
13
14
15
16
17
18
19
20
21
22
23
24

25 Next, we compared the ICL yields and the selectivity of these ROS-activated DNA alkylating agents with
26 the same type of chemotherapy drugs Chlorambucil and Melphalan. Duplex DNA **30** was incubated with
27 increasing concentrations (200 μM, 500 μM, 1 mM) of Chlorambucil, Melphalan, **9**, or **9** with H₂O₂
28 respectively at 25 °C for 16 h. As shown in figure S3, at all concentrations, **9** induced the fewest ICL yield in
29 the absence of H₂O₂ while the highest ICL yield was observed for **9** with the addition of H₂O₂. In particular,
30 at the concentration of 1 mM, the ICL yield of **9** (1.7%) was less than one third of those induced by
31 Chlorambucil or Melphalan (5.7% or 4.9% respectively). In contrast, **9** with H₂O₂ induced much higher
32 yield of DNA ICLs than Chlorambucil or Melphalan at the same dose (8 folds more).
33
34
35
36
37
38
39
40
41
42
43
44

45 **Evaluation of cytotoxicity in 60 human cancer cell lines.** Initially, some compounds were tested against
46 60 human cancer cell lines, which was performed at the National Cancer Institute (NCI Developmental
47 Therapeutics Program). The cell lines were derived from different cancers including leukemia,
48 non-small-cell lung cancer, colon cancer, CNS, melanoma, ovarian, renal, prostate, and breast cancer. The
49 procedure can be found at: <https://ntp.niehs.nih.gov/default.htm>. At a single dose of 10 μM, compounds **3-5**, **9**,
50 and **10** induced significant growth inhibition in the 60 cancer cell lines with less than 50% growth
51
52
53
54
55
56
57
58
59
60

percentages for most cell lines (Figure 2 and supporting information S5). In contrast, no obvious cytotoxicity was observed with compounds containing either a strong withdrawing group (**6**) or an amino acid side chain with Boc protecting group (**7** and **8**). This is consistent with our chemistry observation that **6-8** are poor H₂O₂-inducible DNA cross-linking agents with less than 9% ICL products. To our surprise, **11** with strong cross-linking capability did not show any activity towards these cancer cell lines. Among the active compounds, boronic acids **9** and **10** showed much higher growth-inhibitory effect than the boronic acid esters **3-5**. It is worth noting that although **10** didn't show the best DNA cross-linking efficiency, it exhibited the most significant cytotoxicity towards most of the cell lines tested. For examples, the negative growth percentages (-11% to -23%) were observed with **10**-treated cancer cell lines (Figure 2), such as SR, MOLT-4, HL-60, SF-539, CAKI-1, and MDA-MB-468, indicating that **10** not only inhibited cancer cell growth but led to cancer cell death. However, such phenomena was not observed with other compounds at the same dose. These results suggested that DNA cross-linking ability might not be the only parameter that affect the cytotoxicity and efficacy of these compounds. Introduction of an amino acid side chain and/or boronic acid group may improve the drug-like properties of these compounds.

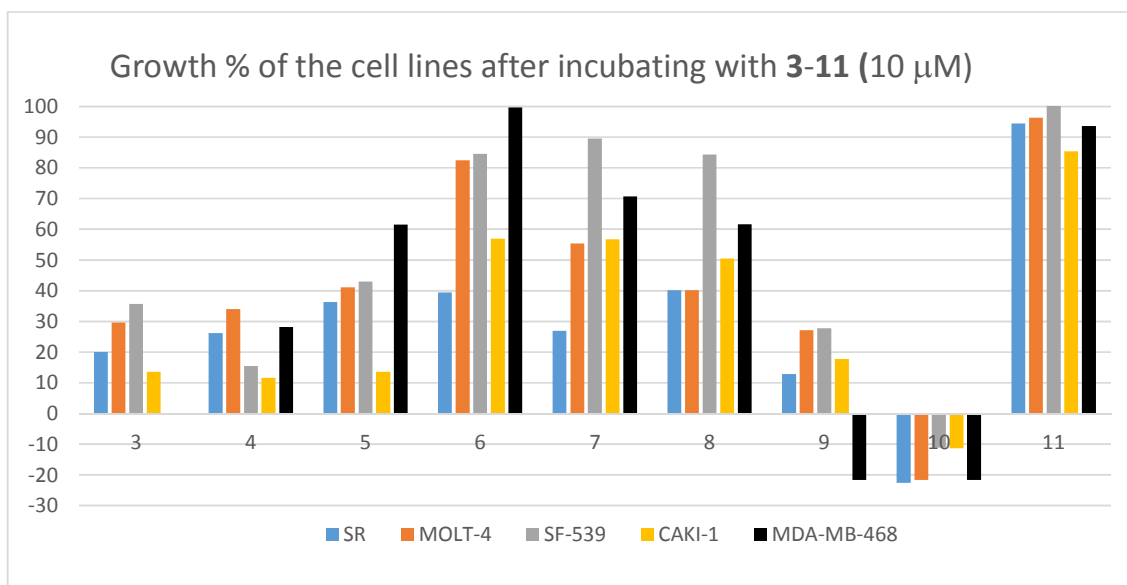


Figure 2. Comparison of cellular activity of **3-11** at the concentration of 10 μM. 60 human tumor cell lines representing leukemia, melanoma, and cancers of the lung, colon, brain, ovary, breast, prostate, and kidney were incubated with 10 μM of **3-11** for 48 h at 37°C, 5 % CO₂, 95 % air, and 100 % relative humidity. The One-dose data is reported as a mean graph of the percent growth of treated cells. The number reported is growth relative to the no-drug control, and relative to the time zero number of cells.

The GI₅₀ of **3**, **4**, **9**, and **10** was further evaluated against the 60 human cancer cell lines at five concentration levels (supporting information S5). Consistent with the data obtained from one dose screening, **10** exhibited the lowest GI₅₀ in most cancer cell lines, such as CCRF-CEM, K-562, MOLT-4, RPMI-8226, SR, HOP-92, HT-29, SNB-75, NALME-3M, IGROV1, and MDA-MB-468. Most of the cancer cell lines that are sensitive to these compounds belong to leukemia or breast cancer cells that proliferate under conditions of oxidative stress and have high intracellular concentrations of ROS (e.g. superoxide, peroxides, and hydroxyl radicals).¹⁸ The boronic acid analogue **9** is slightly more toxic than the pinacol ester **3**. Compound **10** with an amino acid chain is 1.7 to 18 folds more toxic than the parent compound **9**, 2.3 to 9.4 folds more toxic than **3**, and 1.7 to 23.8 folds more toxic than **4**. Although **10** is not the most powerful DNA cross-linking agent, the presence of the amino acid ester chain improves the biophysical properties such as solubility and permeability therefore making it the best drug-like molecule (Table 2). The boronic acids (**9** and **10**) with higher activity have better solubility in PBS (328 μM for **9** and 231 μM for **10**) than **3-5** (24 μM to 167 μM).

Among these agents tested, although compound **10** with an amino ester chain didn't show the highest ICL yield in the presence of hydrogen peroxide, the in vitro results demonstrated that this molecule showed the highest inhibition ability towards most cancer cell lines. We are aware of that cellular activity is also related to drug delivery and is more complex than DNA cross-linking capability. Nevertheless, the investigation of the H₂O₂-induced DNA cross-linking ability and selectivity gave us a good sign that these agents are potential anticancer reagents, which encourage us to continue the further study.

Table 1. GI₅₀ of compounds **3**, **4**, **9**, and **10**.^a

Tumor type	Cell Line	GI ₅₀ (μM)			
		3	4	9	10
leukemia	CCRF-CEM	3.34	2.90	3.27	0.54
	K-562	17.2	5.48	15.8	3.25
	MOLT-4	3.48	2.60	2.90	0.6
	RPMI-8226	10.9	12.0	8.59	2.62
	SR	0.63	0.49	0.48	0.28
non-small-cell lung	HOP-92	9.24	13.3	10.5	0.56

colon cancer	HT-29	13.8	14.7	11.9	4.03
CNS	SNB-75	7.98	10.1	3.21	0.85
melanoma	MALME-3M	17.5	13.6	19.7	2.39
Ovarian	IGROV1	15.6	16.1	18.1	3.32
	SK-OV-3	8.03	4.62	3.81	1.46
Breast Cancer	MDA-MB-468	1.60	7.88	0.51	1.49
	MCF	4.12	3.86	1.89	0.72
^a 60 human tumor cell lines were incubated with 5-dose (100 μ M, 10 μ M, 1 μ M, 100 nM, and 10 nM) of compounds 3 , 4 , 9 and 10 for 48 h at 37°C, 5 % CO ₂ , 95 % air, and 100 % relative humidity. The number reported for 5-dose assay is growth relative to the no-drug control, and relative to the time zero number of cells which is the same as one-dose assay.					

Table 2. Biophysical properties of **3-5**, **9** and **10**.

	3	4	5	6	9	10
Solubility (μ M) ^a	167	24	50	380	328	231
Permeability ^b	-6.31	-	-6.34	-6.63	-6.67	-5.38

^aSolubilities were determined in phosphate buffered saline at pH 7.4. ^bPermeabilities were measured using the parallel artificial membrane permeation assay (PAMPA) at neutral pH (pH 7.4). The following permeability standards (log Pe) were used: ranitidine (-8.02 ± 0.074 cm/s) low permeability, carbamazepine (-6.81 ± 0.0011 cm/s) medium permeability, and verapamil (-5.93 ± 0.015 cm/s) high permeability. The solubility and permeability assay conditions reflect conditions required for activity in cell-based assays.

Cytotoxicity comparison of H₂O₂-activated DNA alkylating agents with clinically useful drugs. Given

that these compounds showed significant cytotoxicity in several cancer cell lines, we compared their efficacy with two of the clinically used DNA alkylating agents, chlorambucil and melphalan, which belong to the aromatic nitrogen mustard analogues acting on cancer cells by alkylating DNA. Chlorambucil is a chemotherapy drug for chronic lymphocytic leukemia (CLL)⁴⁵ and melphalan is used for treatment of advanced breast cancer.⁴⁶ Thus, we investigated their effects towards breast cancer MDA-MB-468 cells and primary CLL cells. It was reported that breast cancer cells and CLL cells have high intracellular concentrations of ROS.⁴³ The dose-dependent response analysis with MDA-MB-468 cells showed that among all H₂O₂-activated compounds, **10** was the most cytotoxic compound with an IC₅₀ of 3.43 μ M, which was 10-14 folds more toxic than chlorambucil (IC₅₀ 48.7 μ M) and melphalan (IC₅₀ 34.44 μ M) (Figure 3).

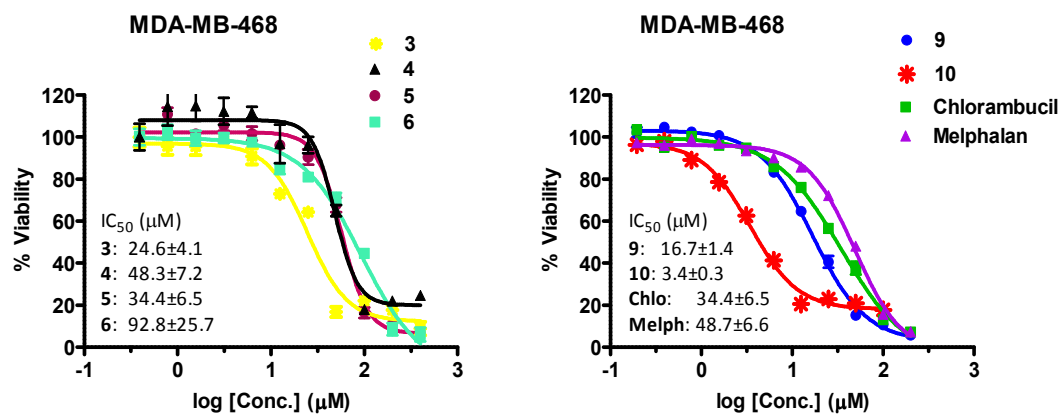


Figure 3. Comparison of inhibition activity of **3-6** and **9-10** with that of chlorambucil and melphalan. The Fluorescence polarization (FP) assay was conducted in 384-well white polystyrene microplates (Corning, #3570). Compounds transfer into 20 μ l assay solution was accomplished using a stainless steel pin tool (V&P Scientific) delivering 200 nl of compound at different concentrations. Incubation time is 48 h. Inhibition of binding was detected by fluorescence polarization using a M1000, Tecan reader at excitation/emission wavelength of 630/685 nm. IC₅₀ value (μ M) was calculated using the following non-linear regression equation: $Y = \text{Bottom} + (\text{Top} - \text{Bottom}) / (1 + 10^{((\text{LogIC}_{50} - X) * \text{HillSlope}))}$.

Similarly, dose-dependent experiments on evaluation of apoptosis using primary CLL cells with three representative compounds (**5**, **10**, and chlorambucil) side by side in the same patient sample (n=6) demonstrated that **10** is more toxic to CLL lymphocytes than chlorambucil and H₂O₂-activated reagent **5** (Figure 4). The IC₅₀ of **10** in CLL lymphocytes ranged from 3 nM to 778 nM, while for chlorambucil and compound **5** the IC₅₀ were not achieved under the dosages tested. Our previous study showed that the IC₅₀ of the lead compound **9** was 5000-6000 nM, demonstrating less activity than **10** (Note: five samples obtained from five patients were tested. Due to heterogeneous response between samples, the IC₅₀ range was wide)²⁸. Collectively, these data demonstrate that among these compounds, compound **10** is highly potent to induce apoptosis in CLL lymphocytes compared to chemotherapy drugs, indicating this could be the best drug-like molecule.

(A)

(B)

(C)

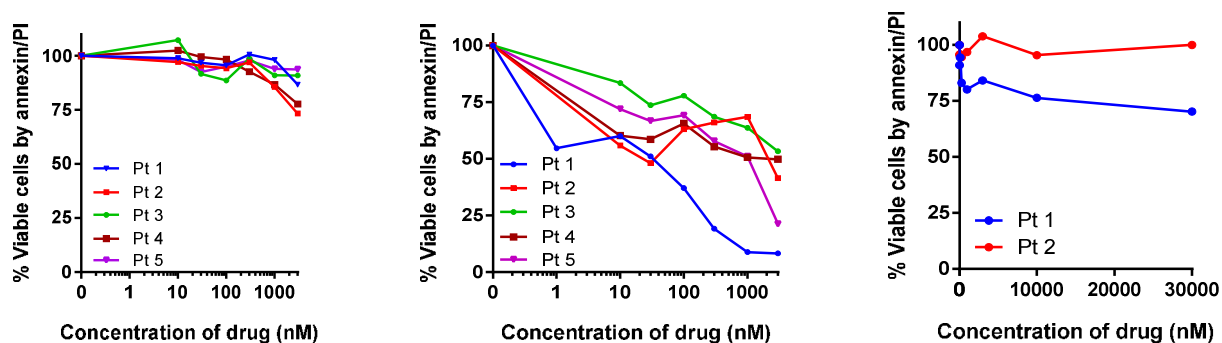


Figure 4. Dose-dependent apoptosis of CLL cells with compounds **5**, **10**, and chlorambucil. CLL lymphocytes were obtained from CLL patients and incubated with series of concentrations of compounds **5**, **10**, and chlorambucil for 24 h, and the apoptosis induction was measured by annexin/PI binding assay: (A) compound **5** (n = 5); (B) compound **10** (n = 5); (C) Chlorambucil (n = 2). Each colored line represents a patient and the data point on the line denotes the concentration of the drug. The survival curve is drawn using GraphPad Prism 6.0.

To evaluate the selectivity of these compounds to cancer cells, normal lymphocytes were tested for toxicity with two representative compounds (**5** and **10**, n=3). The statistical evaluation demonstrated that even at highest concentrations of 10 μ M, no obvious toxicity observed with either compound (Figure 5).

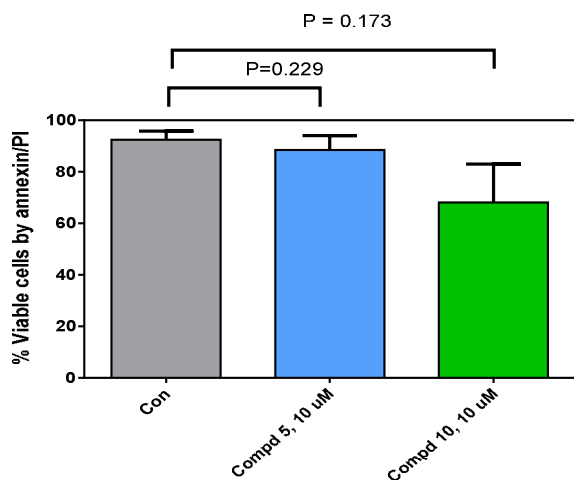
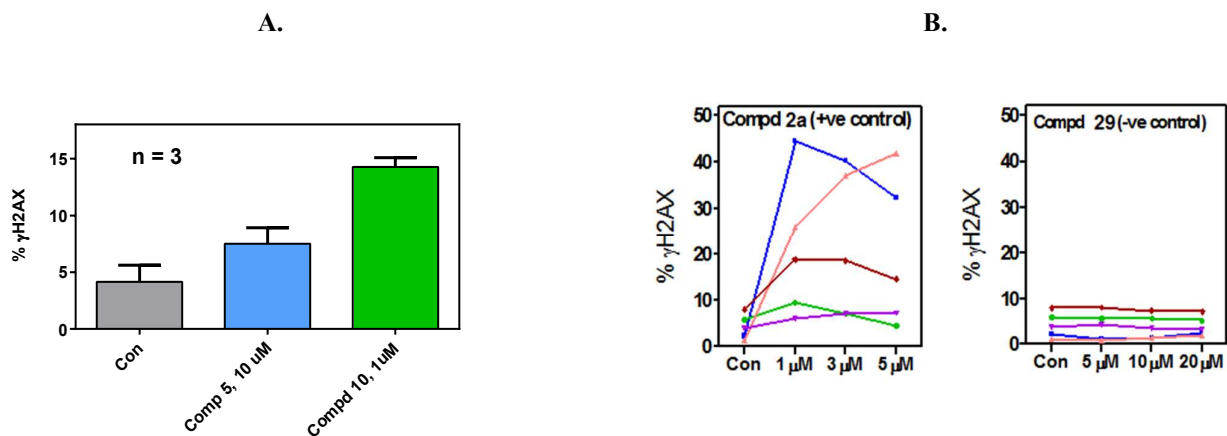
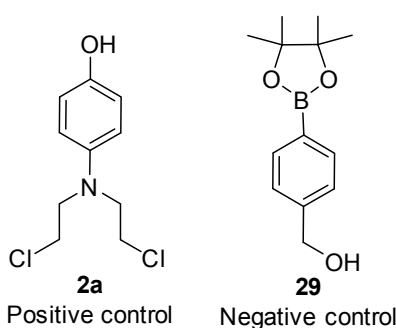


Figure 5. Evaluate apoptosis in normal lymphocytes: Normal PBMCs were obtained from normal donors (n=3) and the toxicity of compounds **5** and **10** (10 μ M) were evaluated by annexin / PI binding method.

Mechanism of action. H2AX is a protein that is responsible for DNA damage repair.⁴⁷ Formation of γ H₂AX is a measure of DNA damage response. One DNA damage, such as DNA strand break or DNA cross-link, leads to 200 phosphorylation of H2AX forming γ H₂AX. The reagent-treated CLL primary cells that were

1 tested for apoptosis were also used to assess H₂AX phosphorylation by flow cytometry. As expected, there
2 was an increase in the γ H₂AX formation in prodrug-treated CLL cells (Figure 6; n=3). Among 3 compounds
3 tested on the CLL leukemic lymphocytes from 3 subjects, **10** led to the most severe DNA damage as well as
4 apoptosis because the maximum H₂AX phosphorylation was observed for **10**-treated CLL cells. Compound
5
6 tested on the CLL leukemic lymphocytes from 3 subjects, **10** led to the most severe DNA damage as well as
7 apoptosis because the maximum H₂AX phosphorylation was observed for **10**-treated CLL cells. Compound
8
9
10 **2a**, a positive control, also led to an increase in H₂AX phosphorylation in **2a**-treated CLL cells, while **29** (a
11
12 negative control) did not have such effect on CLL cells. Collectively these data are consistent with our
13
14 hypothesis.
15
16
17
18



45
46 **Figure 6.** Induction of DNA damage response measured by H₂AX phosphorylation. **A.** CLL lymphocytes
47 (n=3) were incubated with compounds **5** (10 μ M) and compound **10** (1 μ M); **B.** CLL lymphocytes (n=5) were
48 incubated with **2a** and **29** at increasing concentrations (5 – 20 μ M) for 24 hrs and H₂AX phosphorylation was
49 measured by flow cytometry.
50

51
52 **In vivo efficacy of the ROS-activated anticancer reagents.** Suspension cells like lymphocytes often show
53 a higher sensitivity to chemotherapeutics due to their higher exposure in solution when compared to
54 adherent cancer cells. Therefore, we focus on MDA-MB-468 cell line and use them for *in vivo* breast cancer
55
56
57
58
59
60

xenograft. Toxicity study with mice showed that no obvious toxicity was observed for **10** within three months period when the mice were injected with 1.5 mg /kg of **10** per day and 5 days per week. Thus, a dosage of 1.5 mg/kg was used for determining the *in vivo* efficacy of **10** in a MDA-MB-468-derived xenograft mouse model. Tumor-bearing mice were treated i.p. with vehicle or **10** (1.5 mg/kg) (Figure 7). All mice were weighed regularly and the tumor size measured using a caliper every week. After 7 weeks of treatment, tumor sizes in **10**-treated mice ranged from 58% to 170% of the initial size (Figure 7A). In contrast, the control mice showed significant tumor growth, reaching 278%-657% of the original tumor size in that period. Normal increase of body weight was observed for all mice (Figure 7B). Together, these results indicated that **10** efficiently suppressed tumor growth in mice without obvious side effects.

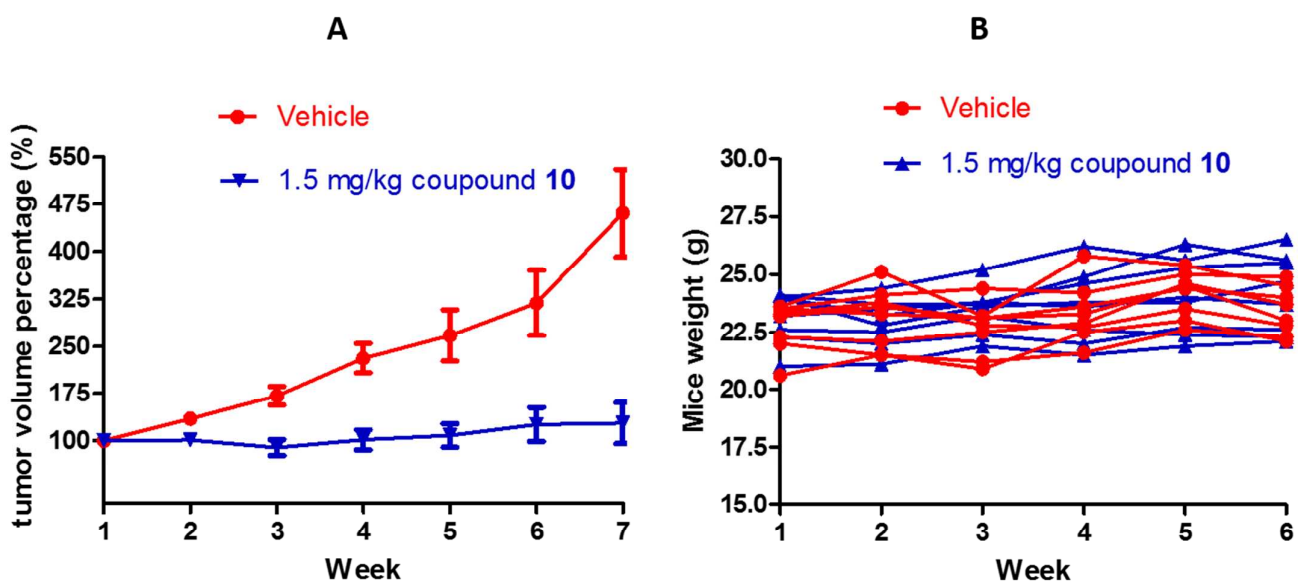


Figure 7. Compound **10** inhibits tumor growth in athymic nude mice. A dosage of 1.5 mg/kg was used for determining the *in vivo* efficacy of **10** in a MDA-MB-468-derived xenograft mouse model. Tumor-bearing mice were treated i.p. with vehicle (DMSO only) or **10** (1.5 mg/kg) (11 mice per group). (A) *In vivo* tumor volumes after injection of DMSO only (control) or 1.5 mg/kg of **10**; (B) comparison of mice weight in DMSO-treated mice and **10**-treated mice.

CONCLUSION

In summary, our investigation of a series of novel aromatic nitrogen mustard arylboronate esters revealed that the aromatic substituents significantly affected their DNA cross-linking ability and cellular activity. A

1 weak electron donating group introduced in the benzene ring increases the selectivity (defined as the ratio of
2
3 ICL yield with H₂O₂ to that without H₂O₂) while a strong donating group or a withdrawing group decreases
4
5 the selectivity. Bulky groups block the interaction between these compounds and DNA therefore inhibiting
6
7 DNA cross-linking and leading to low cellular activity. Introduction of a boronic acid and an amino acid
8
9 side chain greatly improved the solubility and cell membrane permeability, leading to higher cellular activity.
10
11 Compound **10** containing a boronic acid and a cysteine methyl ester side chain showed the highest cellular
12
13 activity towards most cell lines tested. In particular, breast cancer cell lines and leukemia cell lines are
14
15 highly sensitive to **10** that is 10-fold more potent than Mephalan, 14-fold more potent than Chlorambucil
16
17 and 5-fold more potent than the lead compound **9**. Compound **10** exhibited an IC₅₀ of 3 nM to 778 nM
18
19 towards primary CLL cells obtained from peripheral blood of patients, while much higher IC₅₀ was observed
20
21 for the lead compound **9** (IC₅₀ = 5-6 μM) and the IC₅₀ was not achieved for chlorambucil under tested
22
23 dosages. More importantly, compound **10** efficiently inhibited tumor growth in a MDA-MB-468-derived
24
25 xenograft mouse model while no obvious side effects were observed, such as no weight loss and other
26
27 unusual behavior. Normal increase of body weight was observed for both compounds-treated mice and
28
29 control mice. Collectively, these data demonstrated the selectivity and therapeutic utility of these agents,
30
31 which inspires further and effective application as potential cancer chemotherapies.
32
33
34
35
36
37
38
39

40 **EXPERIMENTAL SECTION**

41
42
43 **Chemistry.** Unless otherwise specified, chemicals were purchased from Aldrich or Fisher Scientific and
44
45 were used as received without further purification. T4 polynucleotide kinase was purchased from New
46
47 England Biolabs. Oligonucleotides were synthesized via standard automated DNA synthesis techniques
48
49 using an Applied Biosystems model 394 instrument in a 1.0 μmole scale using commercial 1000 Å
50
51 CPG-succinyl-nucleoside supports. Deprotection of the nucleobases and phosphate moieties and cleavage of
52
53 the linker were carried out under mild deprotection conditions using a mixture of 40% aqueous MeNH₂ and
54
55 28% aqueous NH₃ (1:1) at room temperature for 2 h. [γ-³²P]ATP was purchased from Perkin-Elmer Life
56
57
58
59
60

Sciences. Quantification of radiolabeled oligonucleotides was carried out using a Molecular Dynamics phosphorimager equipped with ImageQuant, version 5.2, software. ^1H NMR and ^{13}C NMR spectra were taken on either a Bruker DRX 300 or DRX 500 MHz spectrophotometer. Silicon reagents were used in CDCl_3 as internal standard. High-resolution mass spectrometry IT-TOF was used for measurement of molecular mass. The purity was determined by RP-HPLC on a 4.6×250 mm RP-C18 column with 254 nm detection, which confirmed that all compounds had $\geq 95\%$ purity. Systematic numbering of chemical structures are shown in support information S7.

***N,N*-Bis(2-chloroethyl)-3-methyl-4-(4,4,5,5-tetramethyl-1,3,2-dioxaborolan-2-yl)aniline (4)**. Step 1. A mixture of 4-bromo-2-methylaniline (0.1 mol), 2-chloroethanol (40 mL), CaCO_3 (20.0 g), and NaI (2.8 g) in 250 mL water was heated to reflux overnight for 24 h, then extracted with dichloromethane and washed with water. After evaporation of the solvent, the residue was purified by column chromatography (Hexane/Ethyl Acetate = 1:2) to afford 2,2'-((4-Bromo-3-methylphenyl)azanediyl)diethanol (**13a**) as a white solid (14.8 g, 55%). mp 46.0-47.5 °C; ^1H NMR ($\text{DMSO-}d_6$, 300 MHz): δ 2.25 (s, 3H, $\text{H}_3\text{-C}(15')$), 3.38 (t, $J = 6.0$ Hz, 4H, $\text{H}_2\text{-C}(10')$, $\text{H}_2\text{-C}(13')$), 3.53 (t, $J = 6.0$ Hz, 4H, $\text{H}_2\text{-C}(9')$, $\text{H}_2\text{-C}(12')$), 3.73 (t, $J = 5.4$ Hz, 2H, $\text{H-O}(11')$, $\text{H-O}(14')$), 6.45 (dd, $J = 3.0$ Hz, $J = 9.0$ Hz, 1H, $\text{H-C}(2')$), 6.65 (d, $J = 3.0$ Hz, 1H, $\text{H-C}(4')$), 7.24 (d, $J = 9.0$ Hz, 1H, $\text{H-C}(1')$); ^{13}C NMR (CDCl_3 , 75 MHz): δ 23.3, 53.6, 58.5, 109.2, 111.5, 114.3, 132.5, 137.5, 147.9; HRMS-ES (m/z) [$\text{M}+\text{H}$] $^+$ calcd for $\text{C}_{11}\text{H}_{16}\text{BrNO}_2$: 274.0425, found: 274.0437.

Step 2. A solution of MsCl (10 mL, 57.5 mmol) in DCM (10 mL) was added dropwise to a mixture of **13a** (10.8 g, 39.7 mmol) and Et_3N (7.5 mL, 57.5 mmol) in dry CH_2Cl_2 (50 mL) at 0 °C. After 30 min, the mixture was extracted with CH_2Cl_2 twice and the combined organic phase was washed with brine water, dried over Na_2SO_4 and then concentrated under vacuum. The residue was used in the next step without any further purification. The residue was dissolved in DMF (40 mL) and LiCl (4 g, 115 mmol) was added. After stirred at 70 °C for 3 h, the mixture was extracted with CH_2Cl_2 and washed with brine water, dried over Na_2SO_4

1 and concentrated under vacuum. The residue was purified by column chromatography (Hexane/Ethyl
2 Acetate = 10:1) to afford 4-Bromo-*N,N*-bis(2-chloroethyl)-3-methylaniline (**14a**) as a white foam (10.5 g,
3 85%). ¹H NMR (CDCl₃, 300 MHz): δ 2.28 (s, 3H, H₃-C(15')), 3.71-3.72 (m, 8H, H₂-C(10'), H₂-C(13'),
4 H₂-C(9'), H₂-C(12')), 6.53 (dd, *J* = 3.0 Hz, *J* = 9.0 Hz, 1H, H-C(2')), 6.75 (d, *J* = 3.0 Hz, 1H, H-C(4')), 7.31
5 (d, *J* = 9.0 Hz, 1H, H-C(1')); ¹³C NMR (CDCl₃, 75 MHz): δ 23.3, 41.5, 52.5, 111.3, 112.1, 114.9, 132.9,
6 138.2, 146.3; HRMS-ES (*m/z*) [M+H]⁺ calcd for C₁₁H₁₄BrNCl₂: 309.3748, found: 309.9759, chlorine
7 isotopic peak [M+H+2]⁺ found 311.9717.

8 Step 3. A solution of **14a** (1.6 g, 5.2 mmol) in dry THF (60 mL) was cooled to -78 °C under Ar. ⁿBuLi (8.0
9 mL, 2.6 M in Hexane) was added slowly at the same temperature within 10 min. After 30 min, B(O^{*i*}Pr)₃ (2.9
10 g, 15 mmol) was added. The mixture was allowed to warm to room temperature and stirred overnight, then
11 quenched by NH₄Cl solution at 0 °C. The mixture was extracted with CH₂Cl₂, washed with water, dried over
12 Na₂SO₄ and concentrated under vacuum. The residue was purified by column chromatography
13 (Hexane/Ethyl Acetate = 1:1) to afford white solid (4-(bis(2-chloroethyl)amino)-2-methylphenyl)boronic
14 acid (1.0 g, 70%). ¹H NMR (DMSO-*d*₆+D₂O, 300 MHz): δ 2.36 (s, 3H, H₃-C(19')), 3.70-3.71 (m, 8H,
15 H₂-C(9'), H₂-C(10'), H₂-C(12'), H₂-C(13')), 6.47-6.49 (m, 2H, H-C(2'), H-C(4')), 7.39 (d, *J* = 9.0 Hz, 1H,
16 H₂-C(1')); ¹³C NMR (DMSO-*d*₆+D₂O, 75 MHz): δ 23.3, 41.7, 52.3, 108.6, 113.4, 136.4, 144.7, 147.6;
17 HRMS-EI (*m/z*) [M+H]⁺ calcd for C₁₁H₁₆BNO₂Cl₂: 276.0713, found: 276.0726. To a mixture of
18 (4-(bis(2-chloroethyl)amino)-2-methylphenyl)boronic acid (1.0 g, 3.63 mmol) and magnesium sulfate (1 g)
19 in dry Et₂O (50mL) was added pinacol (857 mg, 7.26 mmol) at room temperature. After stirring overnight,
20 the mixture was concentrated under vacuum and purified by column chromatography (Hexane/Ethyl Acetate
21 = 10:1) to afford a white solid **4** (1.1 g, 85%). mp 89.4-90.2 °C; ¹H NMR (CDCl₃, 300 MHz): δ 1.34 (s, 12H,
22 H₃-C(19'), H₃-C(20') , H₃-C(21'), H₃-C(23')), 2.54 (s, 3H, H₃-C(22')), 3.66 (t, *J* = 6.3 Hz, 4H, H₂-C(10'),
23 H₂-C(13')), 3.77 (t, *J* = 6.3 Hz, 4H, H₂-C(9'), H₂-C(12')), 6.49-6.52 (m, 2H, H-C(2'), H-C(4')), 7.71 (d, *J* =
24 8.1 Hz, 1H, H-C(1')); ¹³C NMR (CDCl₃, 75 MHz): δ 22.9, 24.9, 40.4, 53.2, 82.9, 108.2, 112.9, 138.2, 147.3,
25 26 27 28 29 30 31 32 33 34 35 36 37 38 39 40 41 42 43 44 45 46 47 48 49 50 51 52 53 54 55 56 57 58 59 60

1 148.0; HRMS-ES (m/z) $[M+H]^+$ calcd for $C_{17}H_{26}NO_2Cl_2B$: 358.1500, found: 358.1510, chlorine isotopic
2
3 peak $[M+H+2]^+$ found 360.1467.
4
5
6
7

8 ***N,N*-Bis(2-chloroethyl)-3-methoxy-4-(4,4,5,5-tetramethyl-1,3,2-dioxaborolan-2-yl)aniline (5)**. Step 1.
9

10 2,2'-((4-Bromo-3-methoxyphenyl)azanediy)diethanol (**13b**) was prepared according to representative
11
12 example **13a** from 4-bromo-2-methoxyaniline **12b** (20 g). White solid (14.5 g, 50%); mp 107.0-108.6 °C;
13
14

15 1H NMR ($CDCl_3$, 300 MHz): δ 3.62 (t, $J = 4.8$ Hz, 4H, $H_2-C(10')$, $H_2-C(13')$), 3.88 (t, $J = 4.8$ Hz, 4H,
16
17 $H_2-C(9')$, $H_2-C(12')$), 3.90 (s, 3H, $H_3-C(15')$), 6.76 (d, $J = 8.4$ Hz, 2H, $H-C(2')$, $H-C(4')$), 7.38 (d, $J = 8.4$ Hz,
18
19 1H, $H-C(1')$); ^{13}C NMR ($CDCl_3$, 75 MHz): δ 55.3, 60.5, 108.8, 114.2, 131.9, 146.8; HRMS-ES (m/z)
20
21

22 $[M+H]^+$ calcd for $C_{11}H_{16}BrNO_3$: 290.0380, found: 290.0386.
23
24

25 Step 2. 4-Bromo-*N,N*-bis(2-chloroethyl)-3-methoxyaniline (**14b**) was synthesized from **13b** (11.5 g) in a
26

27 similar procedure to the synthesis of **14a**. White solid (11.4 g, 88%); mp 92-93 °C; 1H NMR ($CDCl_3$, 300
28
29 MHz): δ 3.63-3.68 (m, 4H, $H_2-C(10')$, $H_2-C(13')$), 3.72-3.77 (m, 4H, $H_2-C(9')$, $H_2-C(12')$), 3.90 (s, 3H,
30
31 $H_3-C(15')$), 6.22 (dd, $J = 2.1$ Hz, $J = 9.0$ Hz, 1H, $H-C(2')$), 6.29 (d, $J = 2.1$ Hz, 1H, $H-C(4')$), 7.37 (d, $J = 9.0$
32
33 Hz, 1H, $H-C(1')$); ^{13}C NMR ($CDCl_3$, 75 MHz): δ 40.3, 53.8, 56.2, 97.4, 99.7, 105.9, 133.7, 146.8, 156.9;
34
35

36 HRMS-ES (m/z) $[M+H]^+$ calcd for $C_{11}H_{14}OBrNCl_2$: 325.9700, found: 325.9709, chlorine isotopic peak
37
38 $[M+H+2]^+$ found 327.9685.
39
40
41

42 Step 3. Compound **5** was prepared from **14b** (1.7 g) in a similar procedure to the synthesis of **4**. White solid
43

44 (0.78 g, 40%); mp 107.0-108.2 °C; 1H NMR ($CDCl_3$, 300 MHz): δ 1.35 (s, 12H, $H_3-C(19')$, $H_3-C(20')$,
45
46 $H_3-C(21')$, $H_3-C(23')$), 3.66 (t, $J = 6.3$ Hz, 4H, $H_2-C(10')$, $H_2-C(13')$), 3.78 (t, $J = 6.3$ Hz, 4H, $H_2-C(9')$,
47
48 $H_2-C(12')$), 3.85 (s, 3H, $H_3-C(22')$), 6.16 (d, $J = 2.1$ Hz, 1H, $H-C(4')$), 6.27 (dd, $J = 2.1$ Hz, $J = 8.4$ Hz, 1H,
49
50 $H-C(2')$), 7.62 (d, $J = 8.4$ Hz, 1H, $H-C(1')$); ^{13}C NMR ($CDCl_3$, 75 MHz): δ 24.8, 40.4, 53.5, 56.0, 82.9, 95.1,
51
52
53

54 104.0, 138.8, 150.1, 166.5; HRMS-ES (m/z) $[M+H]^+$ calcd for $C_{17}H_{26}BNO_3Cl_2$: 374.1465, found: 374.1459,
55
56 chlorine isotopic peak $[M+H+2]^+$ found 376.1443.
57
58
59
60

1
2
3 ***N,N*-Bis(2-chloroethyl)-2-nitro-4-(4,4,5,5-tetramethyl-1,3,2-dioxaborolan-2-yl)aniline (6)**. Step 1.

4
5 4-Bromo-*N,N*-bis(2-chloroethyl)-2-nitroaniline (**19**) was prepared from compound **17** (12.1 g) in a similar
6
7 procedure to the synthesis of **14a**. Yellow liquid (11.2 g, 83% for two steps). ¹H NMR (CDCl₃, 300 MHz): δ
8
9 3.49-3.59 (m, 8H, H₂-C(10'), H₂-C(11'), H₂-C(12'), H₂-C(13')), 7.27 (d, *J* = 8.7 Hz, 1H, H-C(2')), 7.62 (dd, *J*
10
11 = 2.4 Hz, *J* = 8.7 Hz, 1H, H-C(1')), 7.88 (d, *J* = 2.4 Hz, 1H, H-C(5')); ¹³C NMR (CDCl₃, 75 MHz): δ 41.4,
12
13 = 55.3, 115.7, 127.5, 128.3, 136.3, 141.9, 145.6; HRMS-ES (*m/z*) [M+H]⁺ calcd for C₁₀H₁₁BN₂O₂Cl₂:
14
15 340.9430, found: 340.9454, chlorine isotopic peak [M+H+2]⁺ found 342.9407.
16
17

18
19 Step 2. A mixture of **19** (1.36 g, 4.0 mmol), bis(pinacolato)diboron (1.0 g, 4.0 mmol), KOAc (0.8 g, 8.0 mol),
20
21 and PdCl₂(dppf) (0.33 g, 0.4 mmol) in dioxane (50 ml) was flushed with argon for 10 minutes and heated to
22
23 reflux overnight under argon. After cooling to room temperature, the mixture was extracted with ethyl
24
25 acetate and washed with brine. The organic layers was collected, dried over Na₂SO₄ and evaporated under
26
27 vacuum, the residue was purified by column chromatography (Hexane/Ethyl Acetate = 10:1) to afford **6** as a
28
29 yellow solid (1.3 g, 84%). mp 56.6-58.6 °C; ¹H NMR (CDCl₃, 300 MHz): δ 1.36 (s, 12H, H₃-C(20'),
30
31 H₃-C(21'), H₃-C(22'), H₃-C(23')), 3.55-3.58 (m, 8H, H₂-C(9'), H₂-C(10'), H₂-C(12'), H₂-C(13')), 7.29 (d, *J* =
32
33 9.1 Hz, 1H, H-C(2')), 7.89 (d, *J* = 9.1 Hz, 1H, H-C(1')), 8.15 (s, 1H, H-C(5')); ¹³C NMR (CDCl₃, 75 MHz): δ
34
35 24.8, 41.2, 54.8, 84.4, 123.4, 132.3, 139.2, 144.0, 144.7; HRMS-ES (*m/z*) [M+H]⁺ calcd for C₁₆H₂₃N₂O₄BCl₂:
36
37 389.1215, found: 389.1204, chlorine isotopic peak [M+H+2]⁺ found 3491.1187.
38
39
40
41
42
43
44
45
46

47 **Methyl**

48
49 **3-((2-(bis(2-chloroethyl)amino)-5-(4,4,5,5-tetramethyl-1,3,2-dioxaborolan-2-yl)benzyl)thio)-2-((tert-bu**
50
51 **toxicarbonyl)amino)propanoate (7)**. Step 1. To a suspension of LiAlH₄ (1.75 g, 46.3 mmol) in dry Et₂O
52
53 (50 mL) cooled at 0 °C, a solution of **20** (15 g, 23.15 mmol) in dry Et₂O (50 mL) was added dropwise in 15
54
55 minutes. The resulting mixture was stirred at room temperature for 2 h and then it was quenched by slowly
56
57
58
59
60

adding EtOAc (50 mL). The reaction mixture was poured into H₂O (300 mL) and extracted with EtOAc (3 x 250 mL). The combined organic layers were washed with brine (200 mL), dried over Na₂SO₄ and evaporated under reduced pressure. The crude product was purified by column chromatography (Hexane/Ethyl Acetate = 1:2) to obtain (2-amino-5-bromophenyl)methanol (**21**) as a white solid (4.28 g, 92%); mp 112-113 °C; ¹H NMR (DMSO-*d*₆, 300 MHz) δ 4.37 (d, *J* = 5.7 Hz, 2H, H₂-C(8')), 5.23-5.26 (m, 3H, H₂-C(9'), H-O(10')), 6.38 (dd, *J* = 2.1 Hz, *J* = 8.4 Hz, 1H, H-C(1')), 6.80 (d, *J* = 2.1 Hz, 1H, H-C(5')), 7.11 (d, *J* = 8.4 Hz, 1H, H-C(2')); ¹³C NMR (CDCl₃, 75 MHz): δ 63.1, 105.8, 114.1, 114.3, 132.3, 141.4, 148.8, 148.9; HRMS-ES (*m/z*) [M+H]⁺ calcd for C₇H₈NOBr: 201.9849, found: 201.9862.

Step 2. 2,2'-((4-Bromo-2-(hydroxymethyl)phenyl)azanediyl)diethanol (**22**) was prepared according to representative example **13a** from compound **21** (20.2 g). White solid (11.6 g, 40%); mp 106-107 °C; ¹H NMR (CDCl₃, 300 MHz): δ 3.14 (d, *J* = 5.1 Hz, 4H, H₂-C(11'), H₂-C(13')), 3.38 (s, 2H, H-O(12'), H-O(15')), 3.64 (d, *J* = 5.1 Hz, 4H, H₂-C(10'), H₂-C(14')), 4.74 (s, 2H, H₂-C(8')), 7.20 (d, *J* = 8.7 Hz, 1H, H-C(2')), 7.44-7.48 (m, 2H, H-C(1'), H-C(5')); ¹³C NMR (CDCl₃, 75 MHz): δ 57.2, 59.4, 62.9, 119.0, 126.6, 132.1, 133.2, 140.9, 149.2; HRMS-ES (*m/z*) [M+H]⁺ calcd for C₁₁H₁₆BrNO₃: 290.0378, found: 290.0386.

Step 3. 4-Bromo-*N,N*-bis(2-chloroethyl)-2-(chloromethyl)aniline (**24**) was prepared from compound **22** (11.5 g) in a similar procedure to the synthesis of **14** from **13**. Oil (10.3 g, 76.5% for two steps); ¹H NMR (CDCl₃, 300 MHz): δ 3.41-3.53 (m, 8H, H₂-C(10'), H₂-C(11'), H₂-C(13'), H₂-C(14')), 4.79 (s, 2H, H₂-C(8')), 7.16 (d, *J* = 8.7 Hz, 1H, H-C(2')), 7.47 (dd, *J* = 2.4 Hz, *J* = 8.4 Hz, 1H, H-C(2')), 7.67 (d, *J* = 2.4 Hz, 1H, H-C(1')); ¹³C NMR (CDCl₃, 75 MHz): δ 41.3, 41.6, 57.1, 119.4, 126.6, 132.7, 134.3, 138.3, 146.5; HRMS-ES (*m/z*) [M+H]⁺ calcd for C₁₁H₁₃BrNCl₃: 343.9349, found: 343.9370, chlorine isotopic peak [M+H+2]⁺ found 345.9114.

Step 4. BocCysOMe (2.37 g, 7.1 mmol) was dissolved in Methanol (50 mL), K₂CO₃ (4.5 g, 32 mmol) and **24** (2.2 g, 6.4 mmol) were added and the reaction flushed with nitrogen. The reaction was stirred at room temperature for 2 hours and then evaporated under vacuum, the residue was extracted with EtOAc (200 mL)

1 and washed with H₂O (200 mL) followed by the same amount of brine. The organic layer was dried
2
3 (MgSO₄), filtered, and concentrated under reduced pressure. The crude product was purified by column
4
5 chromatography (Hexane/Ethyl Acetate = 5:1) to provide
6
7 3-((2-(bis(2-chloroethyl)amino)-5-bromobenzyl)thio)-2-((tert-butoxycarbonyl)amino)propanoate (**25**) as a
8
9 white liquid (2.6 g, 75%). ¹H NMR (CDCl₃, 300 MHz) δ 1.43 (s, 9H, H₃-C(25') , H₃-C(26') , H₃-C(27')),
10
11 2.87-3.04 (m, 2H, H₂-C(17')), 3.36 (t, *J* = 6.0 Hz, 4H, H₂-C(11'), H₂-C(13')), 3.45 (t, *J* = 6.0 Hz, 4H,
12
13 H₂-C(10'), H₂-C(14')), 3.73 (s, 3H, H₃-C(19')), 3.84 (d, *J* = 13.2 Hz, 1H, H-C(8')), 3.90 (d, *J* = 13.2 Hz, 1H,
14
15 H₂-C(10'), H₂-C(14')), 3.73 (s, 3H, H₃-C(19')), 3.84 (d, *J* = 13.2 Hz, 1H, H-C(8')), 3.90 (d, *J* = 13.2 Hz, 1H,
16
17 H-C(8')), 4.53-4.55 (m, 1H, H-C(18')), 5.40 (d, *J* = 7.8 Hz, 1H, H-N(20')), 7.09 (d, *J* = 8.4 Hz, 1H, H-C(2')),
18
19 7.33 (dd, *J* = 2.1 Hz, *J* = 8.4 Hz, 1H, H-C(1')), 7.53 (d, *J* = 2.1 Hz, 1H, H-C(5')); ¹³C NMR (CDCl₃, 75
20
21 MHz): δ 28.3, 31.7, 35.1, 41.6, 52.5, 52.6, 53.2, 56.9, 57.2, 80.1, 118.9, 126.6, 131.4, 133.8, 138.3, 146.7,
22
23 155.2, 171.5; HRMS-ES (*m/z*) [M+H]⁺ calcd for C₂₀H₂₉BrCl₂N₂O₄S: 543.0472, found: 543.0481, chlorine
24
25 isotopic peak [M+H+2]⁺ found 545.0459.

26
27
28
29
30 Step 5. A mixture of **25** (542 mg, 1.0 mmol), bis(pinacolato)diboron (500 g, 2.0 mmol), KOAc (167 mg, 1.7
31
32 mmol), and PdCl₂(dppf) (165 mg, 0.2 mmol) in dioxane (25 ml) was flushed with argon for 10 minutes and
33
34 heated to reflux for 5 h under argon. After cooling to room temperature, the mixture was extracted with ethyl
35
36 acetate and washed with brine. The organic layers was collected, dried over Na₂SO₄ and evaporated under
37
38 vacuum, the residue was purified by column chromatography (Hexane/Ethyl Acetate = 5:1) to afford **7** as a
39
40 yellow oil (460 mg, 78%). ¹H NMR (CDCl₃, 300 MHz): δ 1.31 (s, 12H, H₃-C(32'), H₃-C(33'), H₃-C(34'),
41
42 H₃-C(35')), 1.43 (s, 9H, H₃-C(25') , H₃-C(26') , H₃-C(27')), 2.99-3.00 (m, 2H, H₂-C(17')), 3.41-3.49 (m, 8H,
43
44 H₂-C(11'), H₂-C(13') , H₂-C(10'), H₂-C(14')), 3.74 (s, 3H, H₃-C(19')), 3.87 (d, *J* = 11.7 Hz, 1H, H-C(8')),
45
46 3.94 (d, *J* = 11.7 Hz, 1H, H-C(8')), 4.54-4.56 (m, 1H, H-C(18')), 5.43 (d, *J* = 7.8 Hz, 1H, H-N(20')), 7.19 (d,
47
48 *J* = 8.4 Hz, 1H, H-C(2')), 7.67 (d, *J* = 8.4 Hz, 1H, H-C(1')), 7.79 (s, 1H, H-C(5')); ¹³C NMR (CDCl₃, 75
49
50 MHz): δ 25.0, 28.3, 32.5, 35.4, 41.5, 52.5, 53.3, 56.7, 80.0, 83.8, 123.7, 134.6, 134.9, 137.9, 150.3, 155.2,
51
52 171.6; HRMS-ES (*m/z*) [M+H]⁺ calcd for C₂₆H₄₁BBBrCl₂N₂O₆S: 591.2218, found: 591.2233, chlorine
53
54
55
56
57
58
59
60

1 isotopic peak $[M+H+2]^+$ found 593.2188.

2
3
4
5 **(3-(((2-Amino-3-methoxy-3-oxopropyl)thio)methyl)-4-(bis(2-chloroethyl)amino)phenyl) boronic acid**

6 **(10)**. 500 mg of compound **7** was dissolved in 5 mL of DCM, 0.6 mL of trifluoroacetic acid was added via a
7
8 syringe within 10 min. The mixture was allowed to stir overnight and evaporated under vacuum. The residue
9
10 was dissolved in a solution of DCM (20 mL) and H₂O (20 mL) and neutralized with K₂CO₃ (1 M) to pH 6-7.
11
12 The mixture was extracted with DCM and washed with brine. The organic phase was collected and
13
14 concentrated. The crude products were purified by column chromatography (Hexane/Ethyl Acetate = 1:1
15
16 then DCM/MeOH = 20:1) to afford a white foam **10** (90 mg, yield = 26%). ¹H NMR (DMSO-*d*₆/D₂O = 9/1,
17
18 300 MHz): δ 2.73-2.78 (m, 2H, H₂-C(17')), 3.37 (t = 6.3 Hz, 4H, H₂-C(11'), H₂-C(13')), 3.54 (t = 6.3 Hz, 4H,
19
20 H₂-C(10'), H₂-C(14')), 3.59 (s, 3H H₃-C(19')), 3.87 (s, 2H, H₂-C(8')), 7.24 (d, *J* = 8.1 Hz, 1H, H-C(2')), 7.63
21
22 (d, *J* = 8.1 Hz, 1H, H-C(1')), 7.76 (s, 1H, H-C(5')); ¹³C NMR (DMSO-*d*₆/D₂O = 9/1, 75 MHz): δ 32.1, 37.1,
23
24 42.5, 52.3, 54.2, 55.9, 123.9, 134.3, 134.5, 137.3, 150.3, 174.7; HRMS-ES (*m/z*) $[M+H]^+$ calcd for
25
26 C₁₅H₂₄BCl₂N₂O₄S: 409.0921, found: 409.0925, chlorine isotopic peak $[M+H+2]^+$ found 411.0915.
27
28
29
30
31
32
33
34
35
36

37 **(R)-2-Amino-3-(1-(2-(bis(2-chloroethyl)amino)-5-boronobenzyl)-1H-indol-3-yl)propanoic acid (11)**.

38
39 Step 1. NaH (75 mg, 60% in mineral oil) was added to a solution of **27** (560 mg, 1.56 mmol) in anhydrous
40
41 DMF (10 mL) at 0 °C. After the mixture was stirred for 30 min at the same temperature, **24** (532 mg, 1.56
42
43 mmol) in DMF (2 mL) was added slowly. The reaction was allowed to stir at room temperature overnight.
44
45 The mixture was extracted with DCM and washed with brine. The organic phase was collected and
46
47 concentrated to get the crude product which was further purified by column chromatography (Hexane/Ethyl
48
49 Acetate = 5:1), yielding (R)-tert-Butyl
50
51 3-(1-(2-(bis(2-chloroethyl)amino)-5-bromobenzyl)-1H-indol-3-yl)-2-((tert-butoxycarbonyl)amino)propanoat
52
53 e (**28**) as a white solid (700 mg, 65%). mp 69-71 °C; ¹H NMR (DMSO-*d*₆, 300 MHz): δ 1.33 (s, 9H, Boc
54
55
56
57
58
59
60

(27')), 1.34 (s, 9H, ^tBu (28')), 2.98-3.16 (m, 2H, H₂-C(25')), 3.44 (t, *J* = 6.6 Hz, 4H, H₂-C(10'), H₂-C(11')), 3.67 (t, *J* = 6.6 Hz, 4H, H₂-C(9'), H₂-C(12')), 4.14-4.17 (m, 1H, H-C(26')), 5.51 (s, 2H, H₂-C(14')), 6.54 (s, 1H, H-C(20')), 7.03-7.13 (m, 3H, H-C(23') , H-C(1') , H-C(2')), 7.21 (s, 1H, H-C(5')), 7.28 (d, *J* = 7.8 Hz, 1H, H-C(22')), 7.35 (d, *J* = 8.4 Hz, 1H, H-C(21')), 7.42 (dd, *J* = 2.4 Hz, *J* = 8.7 Hz, 1H, H-C(24')), 7.57-7.60 (m, 1H, H-NBoc); ¹³C NMR (CDCl₃, 75 MHz): δ 28.0, 28.4, 41.5, 45.5, 54.8, 56.5, 79.5, 81.8, 109.4, 110.4, 119.4, 119.6, 122.1, 126.0, 126.5, 128.7, 131.2, 131.6, 136.6, 138.2, 145.4, 171.2; HRMS-ES (*m/z*) [M+H]⁺ calcd for C₃₁H₄₀N₃O₄Cl₂: 668.1652, found: 668.1616, chlorine isotopic peak [M+H+2]⁺ found 670.1605.

Step 2. A mixture of **28** (500 mg, 0.75 mmol), bis(pinacolato)diboron (380 g, 1.5 mmol), KOAc (150 mg, 1.5 mmol), and PdCl₂(dppf) (55 mg, 0.075 mmol) in dioxane (25 ml) was flushed with argon for 10 minutes and heated to reflux for 24 h under argon. After cooling to room temperature, the mixture was extracted with ethyl acetate and washed with brine. The organic layers was collected, dried over Na₂SO₄ and evaporated under vacuum, the residue was purified by column chromatography (Hexane/Ethyl Acetate = 5:1) to afford (R)-tert-Butyl

3-(1-(2-(bis(2-chloroethyl)amino)-5-(4,4,5,5-tetramethyl-1,3,2-dioxaborolan-2-yl)benzyl)-1H-indol-3-yl)-2-((tert-butoxycarbonyl)amino)propanoate (**8**) as a white solid (350 mg, 66%). mp 69-71 °C; ¹H NMR (DMSO-*d*₆, 300 MHz): δ 1.19 (s, 12H, H₃-C(33'), H₃-C(34'), H₃-C(35') , H₃-C(36')), 1.31 (s, 9H, Boc (29')), 1.34 (s, 9H, ^tBu (27')), 2.97-3.15 (m, 2H, H₂-C(25')), 3.44 (t, *J* = 11.7 Hz, 4H, H₂-C(10'), H₂-C(11')), 3.62 (t, *J* = 11.7 Hz, 4H, H₂-C(9'), H₂-C(12')), 4.06-4.11 (m, 1H, H-C(26')), 5.46 (s, 2H, H₂-C(14')), 6.98 (d, *J* = 7.8 Hz, 1H, H-C(2')), 7.02-7.13 (m, 4H, H-C(22') , H-C(23') , H-C(25') , H-C(5')), 7.30 (d, *J* = 7.8 Hz, 1H, H-C(21')), 7.38 (d, *J* = 7.8 Hz, 1H, H-C(24')), 7.55-7.58 (m, 2H, H-NBoc, H-C(1')); ¹³C NMR (DMSO-*d*₆, 75 MHz): δ 25.0, 28.6, 28.0, 40.5, 45.3, 55.3, 55.8, 78.6, 80.7, 84.0, 110.4, 110.6, 119.4, 119.2, 121.8, 123.8, 128.0, 128.2, 134.3, 134.5, 135.0, 136.9, 150.5, 155.8, 171.8; HRMS-ES (*m/z*) [M+H]⁺ calcd for C₃₇H₅₂N₃O₆BCl₂: 716.3405, found: 716.3390, chlorine isotopic peak [M+H+2]⁺ found 718.3359.

Step 3. 200 mg of compound **8** was dissolved in 4 mL of DCM, 0.6 mL of trifluoroacetic acid was added via

1 a syringe within 10 min. The mixture was allowed to stir overnight and evaporated under vacuum. The
2
3 residue was dissolved in a solution of DCM (20 mL) and H₂O (20 mL) and neutralized with K₂CO₃ (1 M) to
4
5 pH 6.2. The mixture was extracted with DCM and washed with brine. The organic phase was collected and
6
7 concentrated. The crude products were purified by column chromatography (Hexane/Ethyl Acetate = 1:1
8
9 then DCM/MeOH = 20:1) to afford **11** as a white foam (67 mg, 50%). ¹H NMR (DMSO-*d*₆/D₂O = 9/1, 300
10
11 MHz): δ 3.05 (dd, $J = 9.0$ Hz, $J = 15.0$ Hz, 1H, H-C(25')), 3.05 (dd, $J = 5.0$ Hz, $J = 15.0$ Hz, 1H, H-C(25')),
12
13 3.43 (t = 6.5 Hz, 4H, H₂-C(10'), H₂-C(11')), 3.54-3.57 (m, 1H, H-C(26')), 3.64 (t = 6.5 Hz, 4H, H₂-C(9'),
14
15 H₂-C(12')), 5.42 (d, $J = 16.5$ Hz, 1H, H-C(14')), 5.48 (d, $J = 16.5$ Hz, 1H, H-C(14')), 6.98-7.04 (m, 2H,
16
17 H-C(22') , H-C(23')), 7.09 (s, 1H, H-C(20')), 7.18 (d, $J = 7.5$ Hz, 1H, H-C(2')), 7.26 (s, 1H, H-C(5')), 7.29 (d,
18
19 $J = 7.5$ Hz, 1H, H-C(1')), 7.34-7.66 (m, 2H, H-C(21') , H-C(24')); ¹³C NMR (DMSO-*d*₆/D₂O = 9/1, 75 MHz):
20
21 δ 25.9, 41.4, 44.5, 53.8, 54.2, 88.8, 107.8, 108.9, 117.9, 120.4, 121.9, 126.9, 127.6, 128.1, 132.4, 132.8,
22
23 133.2, 135.5, 147.8, 169.8. HRMS-ES (m/z) [M+H]⁺ calcd for C₂₂H₂₇BCl₂N₃O₄: 478.1466, found: 478.1465,
24
25 chlorine isotopic peak [M+H+2]⁺ found 478.1488.
26
27
28
29
30
31

32 **Detection of DNA cross-linking.** ICL formation and cross-linking yields were analyzed via denaturing
33
34 polyacrylamide gel electrophoresis (PAGE) with phosphorimager analysis. The DNA-DNA cross-linking
35
36 abilities of these compounds were investigated by reacting with a ³²P-labelled 49 mer oligonucleotide
37
38 (Figure 1 and Figure S2) then subjected to 20% denaturing PAGE analysis. The ³²P-labelled oligonucleotide
39
40 (1.0 μ M) was annealed with 1.5 equiv of the complementary strand by heating to 65 °C for 3 min in a buffer
41
42 of 10 mM potassium phosphate (pH 7) and 100 mM NaCl, followed by slow-cooling to room temperature
43
44 overnight. The ³²P-labeled duplex DNA (2 μ L, 1.0 μ M) was mixed with 1.0 M NaCl (2 μ L), 100 mM
45
46 potassium phosphate (2 μ L, pH 8), 10 μ M to 50 mM H₂O₂ (2 μ L) and 10 mM compound (resulted in a
47
48 concentration of 1 mM) and appropriate amount of autoclaved distilled water was added to give a final
49
50 volume of 20 μ L. The reaction mixture was incubated at room temperature for 16 h and then quenched by an
51
52 equal volume of 90% formamide loading buffer. Finally it was subjected to 20% denaturing polyacrylamide
53
54
55
56
57
58
59
60

1 gel analysis.

2
3 **MDA-MB-468 cell line.** The human tumor cell line MDA-MB-468 was cultured in the media (media
4 component: 500 mL of L-15 Leibovitz media (HyClone no: SH30525.01), 50 mL of Fetal bovine serum
5 (MIDSCI no: S01520HI), 5 mL of NEAA (HyClone no: SH30238.01), 5 mL of Penicillin (HyClone no:
6 SV30010). Cells are inoculated into 384-well microtiter plates in 20 μ L at plating densities ranging from
7 5,000 to 10,000 cells/well. After cell inoculation, the microtiter plates were incubated at 37 ° C and 100%
8 relative humidity for 2-3 h prior to the addition of reagents. Reagents are solubilized in dimethyl sulfoxide at
9 20 mM concentration and serially diluted ten times each time 50% decrease in DMSO in a 384-well plate.
10 Then 200 nL of the serially diluted compounds were added to the cell plate (1:100 dilution) by using
11 Freedom EVOware. The plates were incubated for an additional 48 h at 37 °C and 100% relative humidity.
12 Then, 20 μ L of celltiter-Glo Luminescent solutions were added to the cell plates. The plates were further
13 incubated at room temperature for 10 min before the luminescent was measured with Infinite M1000.
14
15
16
17
18
19
20
21
22
23
24
25
26
27
28
29

30 **NCI *in vitro* antitumor screen (IVCLSP).** The IVCLSP of the NCI Developmental Therapeutics Program
31 screens up to 3,000 compounds annually for potential anticancer activity. This program uses 60 human
32 tumor cell lines representing leukemia, melanoma, and cancers of the lung, colon, brain, ovary, breast,
33 prostate, and kidney. In a two-stage screening process, compounds are tested for growth-inhibitory activity
34 in all 60 cell lines at a single dose of 10 μ mol/L, and compounds that achieve a threshold activity are
35 retested in all 60 cell lines in a five-dose screen. The growth-inhibitory activity of a tested compound is
36 expressed as log (GI50, TGI, or LC50), where GI50 is the concentration required to inhibit tumor cell
37 growth by 50%, TGI is the concentration causing total growth inhibition, and LC50 is the lethal
38 concentration at which 50% of cells are killed. For each compound tested, 60 activity values (one for each
39 cell line) make up the activity pattern, or fingerprint, of the compound.
40
41
42
43
44
45
46
47
48
49
50
51
52
53

54 **CLL cells and normal lymphocytes.** Leukemic lymphocytes were isolated from fresh peripheral blood
55 sample obtained from patients with CLL. Separate laboratory protocols were used to obtain blood samples
56
57
58
59
60

1 from patients with CLL and healthy donors. All individuals signed written informed consent forms in
2
3 accordance with the Declaration of Helsinki, and the laboratory protocols approved by the institutional
4
5 review board at the University of Texas MD Anderson Cancer Center. **(A) Isolation of CLL and normal**
6
7 **lymphocytes:** Whole blood was collected in heparinized tubes and diluted 1:3 with cold PBS (0.135 M NaCl,
8
9 2.7 mM KCl, 1.5 mM KH₂PO₄, 8 mM Na₂HPO₄ [pH 7.4]) and layered onto Ficoll-Hypaque (specificgravity,
10
11 1.086; Life Technologies, Grand Island, NY). The blood was then centrifuged at 433 g for 20 minutes, and
12
13 mononuclear cells were removed from the interphase. Cells were washed twice with cold PBS and
14
15 resuspended in 10 mL RPMI 1640, supplemented with 10% autologous plasma. A Coulter channelyzer
16
17 (Coulter Electronics, Hialeah, FL) was used to determine cell number and the mean cell volume. The CLL
18
19 or normal lymphocytes were suspended in medium at a concentration of 1×10^7 cells/mL and fresh cells
20
21 were used for all experiments. **(B) Measurement of apoptosis:** Cell death is evaluated by flow cytometry
22
23 analysis with the use of annexin V–PI double staining. CLL or normal lymphocytes in suspension are
24
25 incubated with 10 μ M of compounds and the cell death was measured by annexin V binding assay. Time
26
27 matched control samples with no compound are also maintained side by side. At the end of incubation time,
28
29 cells are washed with PBS and resuspended in 200 μ L of $1 \times$ annexin binding buffer (BD Biosciences), at a
30
31 concentration of 1×10^6 cells/mL. Annexin V–FITC (5 μ L) is added, and the cells are incubated in the dark for
32
33 15 minutes at room temperature. A total of 10 μ L of PI (50 μ g/mL) is added to the labeled cells and analyzed
34
35 immediately with a FACSCALIBUR cytometer (Becton Dickinson). Data from at least 10000 events per
36
37 sample are recorded and processed using Cell Quest software (Becton Dickinson).
38
39
40
41
42
43
44
45
46

47 **Solubility Assay.** Calibration plots were prepared for each compound for the relationship between solute
48
49 concentration and absorbance using background-subtracted values: In a 384 UV plate (Greiner no. 781801),
50
51 compounds were serially diluted in quadruplicate starting from a 10 mM compound stock solution in DMSO
52
53 (final concentrations: 0 μ M to 300 μ M). Buffer (90 mM ethanolamine, 90 mM KH₂PO₄, 90 mM potassium
54
55 acetate, and 30mM KCl (pH 7.4)) containing 20% acetonitrile was used as the dilution solution. The plate
56
57
58
59
60

1 with the compound solutions was sealed, sonicated for 1 min, and agitated for an additional 5 min before
2 scanning from 230 to 800 nm at 5 min increments. Then, a 384-well filter plate (Part no. 5037) was
3 prewetted with 20% acetonitrile/buffer, and filled with buffer (47.5 μ L) and 10 mM compound in DMSO
4 (2.5 μ L) (The final DMSO concentration was 5%). After sonication (1 min) and agitation (18 h), the
5 mixtures were filtered and 30 μ L of each well was transferred into a 384-well UV plate (Greiner no. 781801),
6 together with the addition of 20 μ L of acetonitrile. The plate was agitated for 5 min and scanned from 230 to
7 800 nm at 5 min increments. The solubility was determined using background-subtracted values and the
8 following equation: solubility = (absorbance at λ_{max})/[(slope)(5/3)]. Each plate had the following solubility
9 standards: 4,5-diphenylimidazole (67.3 \pm 3.7 μ M), β -estradiol (43.0 \pm 2.3 μ M), diethylstilbestrol (108.3 \pm 5.4 μ M),
10 ketoconazole (134.5 \pm 2.4 μ M), and 3-phenylazo-2,6-diaminopyridine (357.7 \pm 7.0 μ M). All experiments were
11 conducted in quadruplicate.

12
13
14
15
16
17
18
19
20
21
22
23
24
25
26
27 **Permeability Assay.** This assay was carried out using Millipore's Multiscreen protocol AN1725EN00. Each
28 plate had the following standards with the following permeability values (logPe): Ranitidine (-8.02 ± 0.074
29 cm/s) represents low permeability. Carbamazepine (-6.81 ± 0.0011 cm/s) represents medium permeability,
30 and verapamil (-5.93 ± 0.015 cm/s) represents high permeability. All experiments were conducted in triplet.
31 See support information section **10** for standard operating procedure of permeability study.

32
33
34
35
36
37
38
39 **In vivo Experiments.** The toxicity and efficacy of **10** was evaluated further *in vivo* under an IACUC approved
40 protocol 14-15 #02. *Safety study:* A maximal tolerated dose (MTD) for **10** was determined with female CD1
41 mice weighing 20-22 g (25-27 days, Charles River Strain Code 022). Compound **10** was formulated in a
42 mixture of 5%-10% propylene glycol, 1-5% Tween, and saline. The maximum volume for ip injection is 100
43 μ L. This was defined as the highest dose not causing a serious adverse event (e.g. death, convulsion, ataxia,
44 aberrant behavior, evident pain observed within 15 minutes of observation). About 18 mice were used with
45 escalating i.p. dosages that was continued until serious adverse events were observed or the maximum dosage
46 is reached (100 mg/kg). Once dosing is complete, animals were observed for 2 days. The longer periods are
47
48
49
50
51
52
53
54
55
56
57
58
59
60

1 used in order to reveal any delayed onset toxicity. Animals with the following signs were euthanized: weight
2
3 loss of 20% from the initial weight or more; the inability to rise or ambulate or to reach food and water over
4
5 three days; and the presence of labored respiration. *Efficacy study:* For mice xenografts, immune-deficient
6
7 female nude mice (35 days, Charles River Strain Code 490) weighing 20-22 g, are anesthetized with
8
9 isoflurane and injected with 2 million cancer cells (MDA-MB-468) suspended in 1:1 solution of matrigel and
10
11 DMEM media (Isoflurane is used to knock the mice out for a few seconds for injection of the cancer cells in
12
13 the desired position). All cancer cells were obtained from ATCC and are negative for blood-borne pathogens
14
15 (viruses). The SC injection (100 uL) occurred in the left or right flank of the mice. Animals were watched
16
17 every day for palpable tumors and animal weight were recorded weekly before the compound treatment.
18
19 Compound was formulated in a similar way for safety study. The maximum volume for ip injection is 100 uL
20
21 at a concentration of 1.5 mg/kg for compound **10**. Briefly, mice with palpable tumors were treated with
22
23 formulated compound in PBS/ PEG400 /DMSO (19:19:2) or vehicle (11 mice per group). Mice were
24
25 weighed daily and tumor size measured using a caliper every 7 days. At the end of the study all tumors were
26
27 harvested and weighed (an individual mouse would be euthanized and tumor excised if the tumor size
28
29 reaches 20 mm in any dimension).
30
31
32
33
34
35
36
37
38
39

40 ASSOCIATED CONTENT

41
42
43
44
45 **Supporting Information Available.** Stability of lead compounds in PBS buffer as well as in the presence of
46
47 GSH, phosphorimage autoradiogram of denaturing PAGE image of DNA cross-link assay, DNA
48
49 cross-linking ability of **9** in comparison with that of Chlorambucil and Melphalan, induction of DNA
50
51 damage response measured by H2AX phosphorylation, toxicity of compounds **3-11** at 10 μ M towards 60
52
53 cancer cell lines from NCI and toxicity of compounds **3, 4, 9, and 10** at 5 doses towards 60 cancer cell lines
54
55 from NCI, FTIR spectra, systematic numbering of chemical structures, standard operating procedure of
56
57
58
59
60

1 permeability study. This material is available free of charge via the Internet at <http://pubs.acs.org>.

2
3 Molecular formula strings of final compounds (CSV).

4 5 **Corresponding Author**

6
7
8 *Xiaohua Peng Ph.D.

9
10 Department of Chemistry and Biochemistry, University of Wisconsin Milwaukee, 3210 N. Cramer St.,
11
12 Milwaukee. WI 53211, USA

13
14
15 E-mail: pengx@uwm.edu

16 17 **Author Contributions**

18
19 ⁺ W. Chen and H. Fan are co-first-authors contributing equally to this work.

20 21 22 **Acknowledgment**

23
24
25
26 We are grateful for the financial support for this research from the National Cancer Institute -
27
28 1R15CA152914-01, and CLL-Global Research Foundation Alliance grants, UW System Applied Research
29
30 Grant, Great Milwaukee Foundation (Shaw Scientist Award), and UWM Research Growth Initiative.

31 32 33 **Abbreviations**

34
35
36 ROS, reactive oxygen species; CLL, chronic lymphocytic leukemia cells; ICLs, interstrand cross-links; SR,
37
38 leukemia cells; NCI-H460, non-small cell lung cancer cells; MDA-MB-468, breast cancer cells; NAC,
39
40 N-acetyl cysteine.

41 42 43 **References**

- 44
45
46
47
48
49
50 (1) Noll, D. M.; Mason, T. M.; Miller, P. S. Formation and repair of interstrand cross-links in DNA. *Chem. Rev.* **2006**, *106*,
51 277-301.
52 (2) Rajski, S. R.; Williams, R. M. DNA Cross-linking agents as antitumor drugs. *Chem. Rev.* **1998**, *98*, 2723-2796.
53 (3) Verga, D.; Nadai, M.; Doria, F.; Percivalle, C.; Di Antonio, M.; Palumbo, M.; Richter, S. N.; Freccero, M. Photogeneration
54 and reactivity of naphthoquinone methides as purine selective DNA alkylating agents. *J Am Chem Soc* **2010**, *132*, 14625-14637.
55 (4) Richter, S. N.; Maggi, S.; Mels, S. C.; Palumbo, M.; Freccero, M. Binol quinone methides as bisalkylating and DNA
56 cross-linking agents. *J Am Chem Soc* **2004**, *126*, 13973-13979.
57 (5) Percivalle, C.; La Rosa, A.; Verga, D.; Doria, F.; Mella, M.; Palumbo, M.; Di Antonio, M.; Freccero, M. Quinone methide
58
59
60

generation via photoinduced electron transfer. *J Org Chem* **2011**, *76*, 3096-3106.

(6) Nadai, M.; Doria, F.; Germani, L.; Richter, S. N.; Freccero, M. A photoreactive G-quadruplex ligand triggered by green light. *Chem. Eur. J.* **2015**, *21*, 2330-2334.

(7) Colloredo-Mels, S.; Doria, F.; Verga, D.; Freccero, M. Photogenerated quinone methides as useful intermediates in the synthesis of chiral BINOL ligands. *J Org Chem* **2006**, *71*, 3889-3895.

(8) Wang, P.; Liu, R.; Wu, X.; Ma, H.; Cao, X.; Zhou, P.; Zhang, J.; Weng, X.; Zhang, X. L.; Qi, J.; Zhou, X.; Weng, L. A potent, water-soluble and photoinducible DNA cross-linking agent. *J Am Chem Soc* **2003**, *125*, 1116-1117.

(9) Kuang, Y.; Sun, H.; Blain, J. C.; Peng, X. Hypoxia-selective DNA interstrand cross-link formation by two modified nucleosides. *Chem. Eur. J.* **2012**, *18*, 12609-12613.

(10) Doria, F.; Richter, S. N.; Nadai, M.; Colloredo-Mels, S.; Mella, M.; Palumbo, M.; Freccero, M. BINOL-amino acid conjugates as triggerable carriers of DNA-targeted potent photocytotoxic agents. *J Med Chem* **2007**, *50*, 6570-6579.

(11) Wang, Y.; Liu, S.; Lin, Z.; Fan, Y.; Wang, Y.; Peng, X. Photochemical Generation of Benzyl Cations That Selectively Cross-Link Guanine and Cytosine in DNA. *Org Lett* **2016**, *18*, 2544-2547.

(12) Terceel, M.; Lee, A. E.; Hogg, A.; Anderson, R. F.; Lee, H. H.; Siim, B. G.; Denny, W. A.; Wilson, W. R. Hypoxia-selective antitumor agents. 16. Nitroarylmethyl quaternary salts as bioreductive prodrugs of the alkylating agent mechlorethamine. *J Med Chem* **2001**, *44*, 3511-3522.

(13) Singleton, R. S.; Guise, C. P.; Ferry, D. M.; Pullen, S. M.; Dorie, M. J.; Brown, J. M.; Patterson, A. V.; Wilson, W. R. DNA cross-links in human tumor cells exposed to the prodrug PR-104A: relationships to hypoxia, bioreductive metabolism, and cytotoxicity. *Cancer Res.* **2009**, *69*, 3884-3891.

(14) Patterson, A. V.; Ferry, D. M.; Edmunds, S. J.; Gu, Y.; Singleton, R. S.; Patel, K.; Pullen, S. M.; Hicks, K. O.; Syddall, S. P.; Atwell, G. J.; Yang, S.; Denny, W. A.; Wilson, W. R. Mechanism of action and preclinical antitumor activity of the novel hypoxia-activated DNA cross-linking agent PR-104. *Clin. Cancer Res.* **2007**, *13*, 3922-3932.

(15) Atwell, G. J.; Yang, S.; Pruijn, F. B.; Pullen, S. M.; Hogg, A.; Patterson, A. V.; Wilson, W. R.; Denny, W. A. Synthesis and structure-activity relationships for 2,4-dinitrobenzamide-5-mustards as prodrugs for the Escherichia coli nfsB nitroreductase in gene therapy. *J Med Chem* **2007**, *50*, 1197-1212.

(16) Johnson, K. M.; Parsons, Z. D.; Barnes, C. L.; Gates, K. S. Toward hypoxia-selective DNA-alkylating agents built by grafting nitrogen mustards onto the bioreductively activated, hypoxia-selective DNA-oxidizing agent 3-amino-1,2,4-benzotriazine 1,4-dioxide (tirapazamine). *J Org Chem* **2014**, *79*, 7520-7531.

(17) Di Antonio, M.; Doria, F.; Mella, M.; Merli, D.; Profumo, A.; Freccero, M. Novel naphthalene diimides as activatable precursors of bisalkylating agents, by reduction and base catalysis. *J Org Chem* **2007**, *72*, 8354-8360.

(18) Hong, I. S.; Ding, H.; Greenberg, M. M. Oxygen independent DNA interstrand cross-link formation by a nucleotide radical. *J Am Chem Soc* **2006**, *128*, 485-491.

(19) Hong, I. S.; Greenberg, M. M. DNA interstrand cross-link formation initiated by reaction between singlet oxygen and a modified nucleotide. *J Am Chem Soc* **2005**, *127*, 10510-10511.

(20) Peng, X.; Hong, I. S.; Li, H.; Seidman, M. M.; Greenberg, M. M. Interstrand cross-link formation in duplex and triplex DNA by modified pyrimidines. *J Am Chem Soc* **2008**, *130*, 10299-10306.

(21) Weng, X.; Ren, L.; Weng, L.; Huang, J.; Zhu, S.; Zhou, X.; Weng, L. Synthesis and biological studies of inducible DNA cross-linking agents. *Angew. Chem. Int. Ed. Engl.* **2007**, *46*, 8020-8023.

(22) Veldhuyzen, W. F.; Pande, P.; Rokita, S. E. A transient product of DNA alkylation can be stabilized by binding localization. *J Am Chem Soc* **2003**, *125*, 14005-14013.

(23) Wang, H.; Rokita, S. E. Dynamic cross-linking is retained in duplex DNA after multiple exchange of strands. *Angew. Chem. Int. Ed. Engl.* **2010**, *49*, 5957-5960.

(24) Wu, J.; Huang, R.; Wang, T.; Zhao, X.; Zhang, W.; Weng, X.; Tian, T.; Zhou, X. Fluoride as an inducible DNA cross-linking agent for new antitumor prodrug. *Org Biomol Chem* **2013**, *11*, 2365-2369.

(25) Di Antonio, M.; Doria, F.; Richter, S. N.; Bertipaglia, C.; Mella, M.; Sissi, C.; Palumbo, M.; Freccero, M. Quinone methides tethered to naphthalene diimides as selective G-quadruplex alkylating agents. *J Am Chem Soc* **2009**, *131*, 13132-13141.

(26) Cao, S.; Wang, Y.; Peng, X. ROS-inducible DNA cross-linking agent as a new anticancer prodrug building block. *Chem. Eur. J.* **2012**, *18*, 3850-3854.

(27) Cao, S.; Wang, Y.; Peng, X. The leaving group strongly affects H(2)O(2)-induced DNA cross-linking by arylboronates. *J*

Org Chem **2014**, *79*, 501-508.

(28) Chen, W.; Balakrishnan, K.; Kuang, Y.; Han, Y.; Fu, M.; Gandhi, V.; Peng, X. Reactive oxygen species (ROS) inducible DNA cross-linking agents and their effect on cancer cells and normal lymphocytes. *J Med Chem* **2014**, *57*, 4498-4510.

(29) Chen, W.; Han, Y.; Peng, X. Aromatic nitrogen mustard-based prodrugs: activity, selectivity, and the mechanism of DNA cross-linking. *Chem. Eur. J.* **2014**, *20*, 7410-7418.

(30) Kuang, Y.; Balakrishnan, K.; Gandhi, V.; Peng, X. Hydrogen peroxide inducible DNA cross-linking agents: targeted anticancer prodrugs. *J Am Chem Soc* **2011**, *133*, 19278-19281.

(31) Peng, X.; Gandhi, V. ROS-activated anticancer prodrugs: a new strategy for tumor-specific damage. *Ther Deliv* **2012**, *3*, 823-833.

(32) Wang, Y.; Fan, H.; Balakrishnan, K.; Lin, Z.; Cao, S.; Chen, W.; Fan, Y.; Guthrie, Q. A.; Sun, H.; Teske, K. A.; Gandhi, V.; Arnold, L. A.; Peng, X. Hydrogen peroxide activated quinone methide precursors with enhanced DNA cross-linking capability and cytotoxicity towards cancer cells. *Eur J Med Chem* **2017**, *133*, 197-207.

(33) Szatrowski, T. P.; Nathan, C. F. Production of large amounts of hydrogen peroxide by human tumor cells. *Cancer Res.* **1991**, *51*, 794-798.

(34) Brown, N. S.; Bicknell, R. Hypoxia and oxidative stress in breast cancer. Oxidative stress: its effects on the growth, metastatic potential and response to therapy of breast cancer. *Breast Cancer Res.* **2001**, *3*, 323-327.

(35) Lim, S. D.; Sun, C.; Lambeth, J. D.; Marshall, F.; Amin, M.; Chung, L.; Petros, J. A.; Arnold, R. S. Increased Nox1 and hydrogen peroxide in prostate cancer. *Prostate* **2005**, *62*, 200-207.

(36) Lippert, A. R.; Van de Bittner, G. C.; Chang, C. J. Boronate oxidation as a bioorthogonal reaction approach for studying the chemistry of hydrogen peroxide in living systems. *Acc. Chem. Res.* **2011**, *44*, 793-804.

(37) Daum, S.; Chekhun, V. F.; Todor, I. N.; Lukianova, N. Y.; Shvets, Y. V.; Sellner, L.; Putzker, K.; Lewis, J.; Zenz, T.; de Graaf, I. A.; Groothuis, G. M.; Casini, A.; Zozulia, O.; Hampel, F.; Mokhir, A. Improved synthesis of N-benzylaminoferrocene-based prodrugs and evaluation of their toxicity and antileukemic activity. *J Med Chem* **2015**, *58*, 2015-2024.

(38) Daum, S.; Reshetnikov, M. S. V.; Sisa, M.; Dumych, T.; Lootsik, M. D.; Bilyy, R.; Bila, E.; Janko, C.; Alexiou, C.; Herrmann, M.; Sellner, L.; Mokhir, A. Lysosome-targeting amplifiers of reactive oxygen species as anticancer prodrugs. *Angew. Chem. Int. Ed. Engl.* **2017**, *56*, 15545-15549.

(39) Schikora, M.; Reznikov, A.; Chaykovskaya, L.; Sachinska, O.; Polyakova, L.; Mokhir, A. Activity of aminoferrocene-based prodrugs against prostate cancer. *Bioorg. Med. Chem. Lett.* **2015**, *25*, 3447-3450.

(40) Toyokuni, S.; Okamoto, K.; Yodoi, J.; Hiai, H. Persistent oxidative stress in cancer. *FEBS Lett* **1995**, *358*, 1-3.

(41) Schumacker, P. T. Reactive oxygen species in cancer cells: live by the sword, die by the sword. *Cancer Cell* **2006**, *10*, 175-176.

(42) Zieba, M.; Suwalski, M.; Kwiatkowska, S.; Piasecka, G.; Grzelewska-Rzymowska, I.; Stolarek, R.; Nowak, D. Comparison of hydrogen peroxide generation and the content of lipid peroxidation products in lung cancer tissue and pulmonary parenchyma. *Respir Med* **2000**, *94*, 800-805.

(43) Trachootham, D.; Zhang, H.; Zhang, W.; Feng, L.; Du, M.; Zhou, Y.; Chen, Z.; Pelicano, H.; Plunkett, W.; Wierda, W. G.; Keating, M. J.; Huang, P. Effective elimination of fludarabine-resistant CLL cells by PEITC through a redox-mediated mechanism. *Blood* **2008**, *112*, 1912-1922.

(44) Veni, G. K.; Rao D. B.; Kumar, D. M.; Usha, B.; Krishma, V. M.; Rao, T. R. Clinical evaluation of oxidative stress in women with breast cancer. *Recent Research in Science and Technology* **2001**, *3*, 55-58.

(45) Rai, K. R.; Peterson, B. L.; Appelbaum, F. R.; Koltz, J.; Elias, L.; Shepherd, L.; Hines, J.; Threatte, G. A.; Larson, R. A.; Cheson, B. D.; Schiffer, C. A. Fludarabine compared with chlorambucil as primary therapy for chronic lymphocytic leukemia. *N Engl J Med* **2000**, *343*, 1750-1757.

(46) Henderson, I. C.; Hayes, D. F.; Gelman, R. Dose-response in the treatment of breast cancer: a critical review. *J Clin Oncol* **1988**, *6*, 1501-1515.

(47) Podhorecka, M.; Skladanowski, A.; Bozko, P. H2AX Phosphorylation: its role in DNA damage response and cancer therapy. *J Nucleic Acids* **2010**, *2010*.

Table of Contents Graphic

